UNIVERSITY OF LATVIA

Virgīnija Vītola

ELECTRONIC EXCITATIONS AND PROCESSES IN LONG LASTING LUMINESCENCE MATERIAL $SrAl_2O_4$

DOCTORAL THESIS

Submitted for the Degree of Doctor of Physics

Subfield of Material Physics

Riga, 2018

Promocijas darbs izstrādāts Latvijas Universitātes Cietvielu fizikas institūtā laika posmā no 09. 2016. līdz 11. 2018.

Darbs sastāv no ievada, četrām nodaļām, aizstāvamām tēzēm un literatūras saraksta.

Darba forma: disertācija fizikas nozarē, Materiālu Fizikas apakšnozarē

Darba vadītājs:

- Dr. phys. Krišjānis Šmits, vadošais pētnieks, Cietvielu Radiācijas Fizikas laboratorijas vadītājs, LU Cietvielu Fizikas institūts.

Recenzenti:

1. Dr.habil.phys. **Māris Spriņģis**, LU Cietvielu fizikas institūts
2. Prof., Dr.habil.phys. **Andris Ozols**, RTU Materiālzinātnes un lietišķās ķīmijas fakultāte
3. Dr.phys. **Ilmo Sildos**, Tartu Universitāte, Lāzerspektroskopijas laboratorijas vadītājs

Promocijas darba aizstāvēšana notiks Latvijas Universitātes Fizikas, astronomijas un mehānikas zinātņu nozares promocijas padomes atklātajā sēdē 2019. gada 12. aprīlī plkst. 14:00, Ķengaraga ielā 8, konferenču zālē.

Ar promocijas darbu un tā kopsavilkumu var iepazīties Latvijas Universitātes Bibliotēkā Rīgā, Raiņa bulv. 19.

LU Fizikas, astronomijas un mehānikas specializētās promocijas

padomes priekšsēdētājs Dr.habil.phys. Linards Skuja,

padomes sekretāre Laureta Buševica

Anotācija

Ar Eu un Dy aktivēts $SrAl_2O_4$ ir materiāls, kurš pēc ierosmes ar redzamo vai ultravioleto gaismu uzrāda ilgu un intensīvu pēcspīdēšanu. Plašās pielietojamības energoefektīvos gaismas avotos dēļ materiāls ir plaši pētīts un izmantots. Lai gan $SrAl_2O_4$:Eu,Dy ir pazīstams jau kādu laiku, tomēr vēl ir neskaidrības tā pēcspīdēšanas mehānismā – piemēram, nav noskaidrota koaktivatora Dy loma. Zinātniskās publikācijas par šo jautājumu sniedz pretrunīgus rezultātus.

Šo neskaidrību noskaidrošanai pētīts aktivēts un neaktivēts $SrAl_2O_4$ materiāls plašā temperatūru diapazonā. Tika apskatīti emisijas spektri pie dažādu veidu ierosmēm, luminiscences dzišanas kinētikas, veikti termiski stimulētas luminiscences mērījumi, lai noskaidrotu lādiņnesēju ķerājcentru dabu un enerģētiskos dziļumus.

Darba rezultātā ir ierosināti uzlabojumi pastāvošajiem ilgi spīdošās luminiscences mehānismiem, kas sevī ietver elektronu tunelēšanu no ķērājcentra uz Eu^{3+}, kā arī darbā ir rasti pierādījumi Dy^{4+} eksistencei stroncija aluminātā. Ir novērota arī neaktivēta materiāla luminiscence, kas sastāv no gadījuma piejaukumu - pārejas metālu un pašvielas defektu luminiscences.

Darbā iegūtie rezultāti dod jaunas zināšanas un papildina pastāvošos priekšstatus par ilgi spīdošās luminiscences mehānismiem ar Eu aktivētā stroncija aluminātā. Darba rezultāti arī paver dažas iespējas plašākai ilgstošu luminoforu pielietošanai.

Annotation

Persistent luminescent material $SrAl_2O_4:Eu^{2+},Dy^{3+}$ is widely used and studied for energy efficient applications. However, the mechanism of the persistent luminescence mechanism and the role of co-dopant are not clear and the publications that are available on the mechanism are contradictory.

A study of $SrAl_2O_4:Eu,Dy$; $SrAl_2O_4:Dy$, and undoped $SrAl_2O_4$ material was conducted in order to clarify these ambiguities. Photoluminescence and radioluminescence spectral measurements were conducted at temperatures ranging from 10 K to room temperature. Thermally stimulated luminescence measurements were used to determine the trapping centre composition and depth in these materials.

Improvements for the mechanism of persistent luminescence have been suggested, that involve tunneling of electron from trapping center to Eu^{3+}, and the proof for stable Dy^{4+} existance in strontium aluminate has been presented. Intentionally undoped material luminescence has been observed, consisting of trace impurity and intrinsic defects luminescence.

The results of this work give new knowledge and improve the existing concepts of persistent luminescence in Eu activated strontium aluminates. They also open some possibilities for wider applications of long lasting phosphors.

List of abbreviations

TSL – thermally stimulated luminescence

V_O – oxygen vacancy

V_{Sr} – strontium vacancy

E - energy

RE – rare earth

XRD – X-ray diffraction

XANES – X-ray absorption near edge structure spectroscopy

EPR – electron paramagnetic resonanse

UV – ultraviolet radiation

CCD - charge-coupled device

RT – room temperature

Contents

1. Introduction

1.1 The motivation of work

Long lasting luminescence (known also as persistent luminescence) has many well known applications – for example decorations, toys and emergency signs for cases of power shortage during an emergency, many of them are based on Eu doped strontium aluminates. Recently multiple unexplored fields of application have appeared, therefore intensifying the search for maximally efficient and long lasting luminescent materials. Road marks with luminescent paint are being developed, as well as plasma electrolitic oxidation coatings for protection and decoration. A very intriguing application in persistent luminophores is the in vivo medical imaging using luminescent nanoparticles [1-4].

The knowledge of the processes ongoing in the material are essential to improve the optical properties of the above mentioned long lasting aluminate luminophores for different applications. However details of these processes are not clear, especially the nature and role of defects involved. We are interested in study of defects that are involved in the luminescence process and the posibilities to control them in the process of synthesis in order to obtain the longest afterglow and good thermal stability – so that the material is usable at different temperatures. The scientific literature about the luminescence processes ongoing in the material is not consentaneous – different models exist that could be responsible for the long afterglow and the defects that are involved are not clear. Also, there are very few articles on luminescent properties of undoped material, leaving a possibility for research in this direction. The main motivation for this work was to highlight details of the long lasting luminescence mechanism and to contribute to the knowledge of defects involved.

1.2 The aim of work

The synthesis of maximally efficient alkaline earth aluminate phosphor with a bright afterglow and long afterglow duration is limited with the lack of knowledge about the mechanism governing the persistent luminescence. There is some general knowledge of the process – it must involve some trapping centers and it involves thermally stimulated process, but many details remain unclear. Therefore the aim of this work is to understand more about the persistent luminescence mechanism, including: the nature of the trapping centers, (hole or electron) and their depths, the trapping and detrapping mechanism as well as the origin of the trapping centers and the role of doping with Eu and Dy.

Therefore the following tasks were set:

1. Conduct the experiments for study of $SrAl_2O_4$:Eu,Dy and $SrAl_2O_4$:Dy afterglow dependence on temperature.

This study can contribute in understanding details of afterglow mechanism including the charge transfer process.

2. To record and compare the luminescence spectra under excitation, afterglow spectra and TSL spectra for $SrAl_2O_4$:Eu,Dy and $SrAl_2O_4$:Dy.

The co-activation with Dy increase the intensity and duration of afterglow, however it has not been determined whether it causes creation of new defects or increases the number of previous defects. It is unknown whether Dy is a charge trap.

3. To study the intentionally undoped $SrAl_2O_4$ luminescence and TSL.

The luminescence of undoped $SrAl_2O_4$ was studied rarely and the defects in this undpped composition were not identified. Therefore the study can highlight whether the host defects contribute in afterglow.

4. Summarize and analyze the results obtained in experiments to find out whether they contribute to a more complete understanding of the long-lasting luminescence mechanism.

Execution of each task could contribute to a more complete understanding of the processes that underlie the persistent luminescence. As a result, one of the already known models might be improved, or even a different mechanism could be proposed.

1.3 Contribution of the author and scientific novelty of work

The author has conducted the experiments that are connected with all of the described results except the XRD measurements. The interpretation of the experimental results has been done together with colleagues from Institute of Solid State Physics Radiation laboratory. The author has presented the work in multiple international and local conferences with oral and poster presentations. The author has taken part (as the main author and as one of the co-authors) in the making of scientific publications.

The main results from this research are novel and the analysis of the results has given new knowledge about the ongoing processes in the material. The thesis of this work state novel results that have not yet been discussed before in scientific literature – tunneling luminescence as a part of the persistent luminescence process, proof for stable Dy^{4+} existance in strontium aluminate and observation of luminescence from unactivated $SrAl_2O_4$ material, leading to a conclusion that the F-center luminescence contribute in it.

These results are significant – they give new knowledge and improve the existing concepts of persistent luminescence in Eu activated strontium aluminates. Them also open some possibilities for wider applications of long lasting phosphors.

2. Literature review

2.1 Luminescence

The theory of luminescence and experimental techniques as well as examples of luminescence application are described in a number of textbooks, e.g. [5-7]. Therefore below is short description of only the main features that relate directly to this work.

Luminescence is a general term to describe the process in which a material absorbs energy from an external source and re-emits that energy in the form of visible light. Luminescence is a process that is unrelated to the blackbody radiation, that is defined by the Plancks law. According to the definition of S. Vavilov – luminescence is emission of photons additionally to the thermally emitted ones and the afterglow time greatly exceeds the oscillation period of light waves [6]. There are many types of luminescence classified by the origin of the excitation energy, but this research is focused exclusively on the lumninescence that is created by irradiating the sample with photons. Luminescence is a widely studied phenomenon due to the great applicability – screen lighting, fluorescent lightbulbs, markers and many other devices.

Luminescence can also be classified in two types by the duration of the afterglow. Fluorescence is the type of luminescence that does not exceed 10 ms after the termination of excitation [5]. There are many possible aplications for this type of luminescence, for example, luminescent screens, light bulbs, scintillators etc. However in this research we are interested in the second type of luminescence – phosphorescence which can last from minutes up to several hours after the termination of excitation. The reason why luminescence is delayed, is the presence of charge carrier trapping centers, resulting in slower charge carrier release followed by migration to the luminescence center and thus contributing to a longer afterglow.

Solid state luminophores are crystals or glasses with dopants or activators, that create luminescence centers in the host matrix. In these materials it is usually not the material itself that radiates light (if not talking about exciton and host defects luminescence), but the dopant ions, that act as luminescence centers.

The configurational coordinate model for the energetical states of the system is often used for the explanation of luminescence processes. In Fig. 2.1. two energetical states in the configurational coordinates are presented for an activator ion – the ground state and the excited state. Electron can be promoted in the excited state if the activator absorbs a photon with the appropriate energy. In the excited state the electron has two possible ways: (I) if the temperature of the material is high enough, electron can reach the intersection of the excited and ground state (Fig. 2.1. b) and from there return to the ground state, releasing energy as phonons – that is called luminescence quenching. Otherwise (II) the electron can lose some of its energy for phonon generation, thus electron comes to the lowest point of the excited state and from there return to the ground state by emitting a photon; the emitted photon has lower energy than the one that was absorbed (Fig. 2.1 a). This phenomenon was discovered by G. Stokes and is therefore called the Stokes shift. It is not true for all the cases though – it is possible that the emitted photon has a larger enegy than the one absorbed (for example, in the case of two-photon absorption) and the so called anti-stokes radiation appears.

The quantum efficiency for a phosphorescent material is by definition the ratio of the number of emitted and the number of absorbed photons. For example, if every absorbed photon creates an excitation event and a resulting emission is one photon, the material has a quantum efficiancy of 100%. However in reality many excited luminescence centers will return to the ground state without the emission of a photon (non-radiative transition), making the quantum efficiancy much less then 100%. When the temperature rises, the quantum efficiency of a phospor usually drops due to an increase of the non-radiative transitions.

If a large fraction of the luminescent centers return to the ground state without emission of a photon (non-radiative transitions), the quantum efficiency will be much lower than 100%.

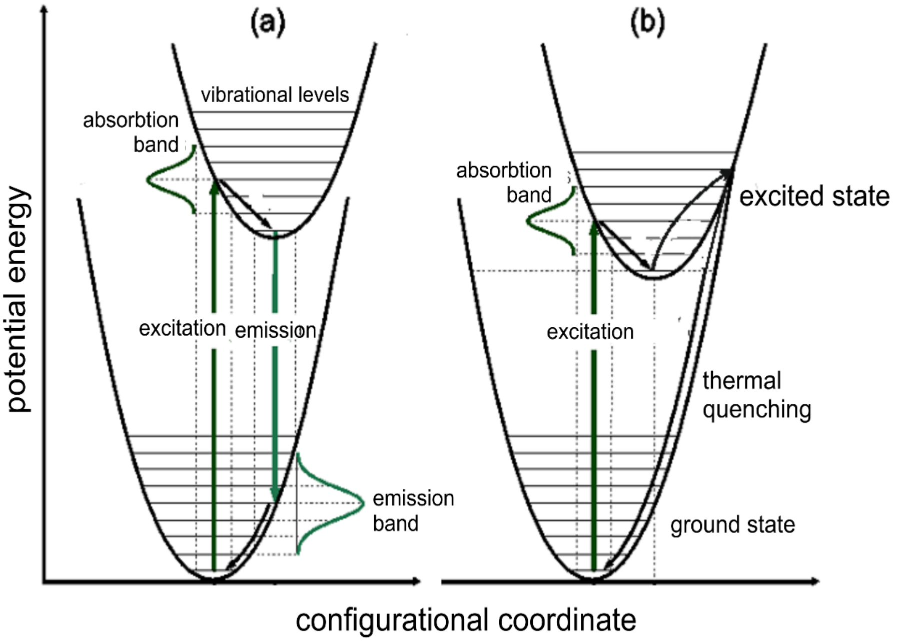

Fig. 2.1. a) excitation followed by emission, that is governed by Stokes law b) excitation followed by luminescence quenching

The band theory of solids is initially based on the research of electronic properties of crystals. In a crystalline solid the atoms or ions are located in a periodic structure and therefore the simplest model is for the electron in a periodic electric field. It turns out that in this model the electron has definite regions of allowed and forbidden energies that are called energy bands. The electron energies in the allowed bands are discrete, but very densely packed, and the number of the energy levels is determined by the number of atoms presented in the system. In the valence band all possible electron states are filled whereas in the conduction band there are free energy levels. These two bands in insulators and semiconductors are separated by a band gap, that has no energy levels in it. In metals, the two bands are overlapping. One must note that with this we are considering the energetical diagram of the whole crystal, not seperate constituents. Electrons in the conduction band are delocalized – they belong to the crystal in whole, not to a certain atom.

In the case if there are no defects or impurities in the crystal lattice of the luminescent material, the band structure consists of only valence, conduction bands and the band gap – there are no energy levels in the band gap. If there are some intrinsic or impurity defects in the host matrix, it may result in some energy levels that are located within the band gap. The impurities and intrinsic defects are dispersed in the host matrix and are located relatively far from one another. That is the reason they do not form energy bands (Fig. 2.2).

Charge carrier trapping centers are defects of the crystal lattice, that contribute an energy level to the band gap – and a charge carrier – electron or hole – can be attracted to such a defect. The trapping centers influence the speed of electron – hole recombination. If there are energetically deep trapping centers for both electrons and holes, the probability for recombination gets very small.

Both impurities and intrinsic defects can serve as trapping centers – vacancies, interstitial atoms or ions, dislocated atoms and other irregularities. One of the reasons a defect can serve as a trapping center is its charge relative to the crystal lattice, for example, Dy^{3+}, when incorporating in the $SrAl_2O_4$ matrix, substitutes for Sr^{2+} and has +1 excess charge, therefore it could be likely to attract an electron. It is also possible, that the impurity, when substituting one of the host atoms (ions), holds equal charge as the host atom – there is no change in charge and the substituant does not hold excess charge to attract the charge carriers with. However – the electronic configuration of the substituent can be different, thus changing the periodic potential of the latticce and possibly becoming a charge carrier trapping center. Under UV or other excitation, some of the charge carriers generated by the excitation become trapped in these localized levels – trapping centers. There is a spatial separation between these trapping centers and the luminescent centers, therefore their orbital wavefunctions might not overlap, meaning that the probability of direct recombination with the luminescence center is very low. There trapped electrons or holes are maintained in a metastable state – until a moment where there is sufficiant energy supply for detrapping them and hence inducing their recombination.[8].

The charge carrier release from trapping centers play an important role in determining the duration of afterglow. One of the main characteristics is the energetical depth of a trapping center – that is the activation energy, that is needed to release a trapped charge. “Shallow” trapping centers – with the energetical depth less than 0.4 eV begin the release of the trapped charges at low temperatures and at room temperatures the lifetime of the afterglow is short. Very “deep” trapping centers with the energetical depth exceeding 2 eV, on the other hand, release the trapped charges only at high temperatures, therefore the trapped charges are stable at room temperature. The lifetime τ of a trapped charge carrier is inversely proportional to the detrapping probability, and depends exponentially on the ratio of the trap depth to the thermal energy, E_T/k_BT. Consequently, at room temperature the lifetime τ, and thus luminescence, is longer when the detrapping requires a higher energy. However, the observation of luminescence by naked eye requires a sufficient luminous flux, i.e., a sufficiently fast detrapping process. [8].

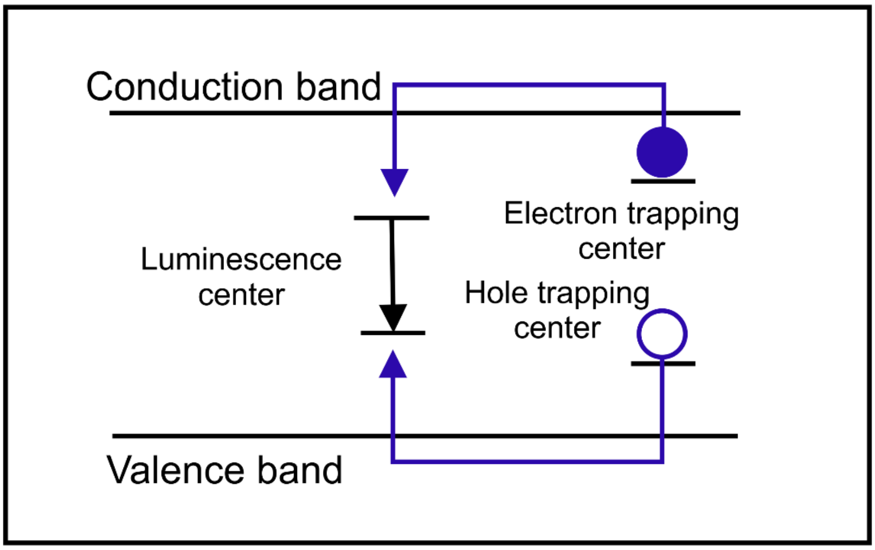

Fig. 2.2. The typical model of phosphorescence involving a luminescence center and charge carrier release from traps. The electrons and holes can be released from the local levels by the means of sufficient thermal energy and can either be de-trapped or reach the luminescence center and recombine.

To observe the long lasting (persistent) luminisence at room temperature, it is necessary that the energetical depth of the charge carrier trapping centres is somewhere between “shallow” and “deep” – ideally around 0.65 eV [5]. The above mentioned is true if the luminescence is governed by thermally stimulated processes – that means the charge carriers are thermally released from the trapping centers with the help of surrounding thermal energy. There are also other processes that might cause the long lasting luminescence, for example, electron tunneling from trap center to luminescence center or energy transfer, and in those cases a different interpretation must be deployed, because the distance from the trapping center to the luminescence center will be of importance rather than the temperature.

Electrons can be promoted to the conduction band from trapping centers when irradiated with light and it is important to note that it occurs at lower excitational energies than needed for the transition valence band-conduction band. Electron that has been promoted to conduction band, loses any connection with the original defect site where it came from and is free to move around in the crystal until it is trapped once more or recombine. If it recombines, the excess energy can be emitted as light (recombination luminescence), (Fig. 2.3).

It is also possible that the activators have ground state level and excited state level within the band gap of host. In this case the absorption of excitation energy can occur without the ionization of the luminescence center. The electron return to the ground state and the resultant emitted light is referred to as intra-center luminescence.

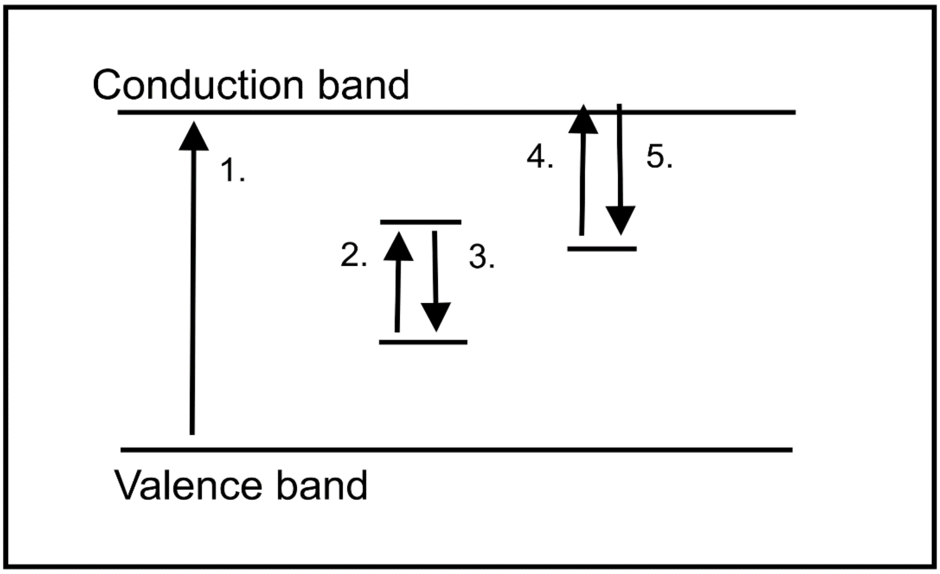

Fig. 2.3. The band scheme for a crystal phosphor with two types of luminescence centers one with a ground state in the band gap and the other with ground state and excited state in the band gap. 1. – electron transition from valence to conduction band with the absorption of excitation light, 2. – excitation of luminescence center, 3. – electron transition to the ground state, 4. – transition from the ground state of luminescence center to conduction band with the absorption of excitation light, 5. – recombination of electron with ionized trapping center .

2.2 Characteristics of luminescence

2.2.1 Long lasting luminescence

The typical profile of luminescence excitation and afterglow is presented in Fig 2.4. The luminescence intensity undergoes a charging phase under excitation. The excitation energy during this phase is spent for luminescence centres excitation and gradual filling of traps. Luminescence intensity reaches the maximum value, that corresponds to the point where recombination rate is the same as excited centre creation rate. After the termination of excitation the second stage is gradual charge release from the trapping centers, that results in excited luminescence centers creation. During second stage the released charges migrate to the luminicence center and in recombination photons are emitted, accounting for this residual luminescence afterglow. As the number of trapped charges decrease, afterglow intensity also decreases. The luminescence kinetics can give us some useful knowledge about the trapping centers. There are multiple mathematical shapes that can describe the afterglow decay shape, that depends on many physical circumstances - trap depth and concentration, retrapping rate (frequency factor), the number of traps and centers involved, temperature, excitation intensity, etc. The possibilities include exponential – as the simplest, single center intrinsic luminescence, hyperbolic for multiple centers, stretched exponential for disordered systems etc, but it frequently turns out that to predict precisely the shape is quite difficult due to the numerous influencing factors.

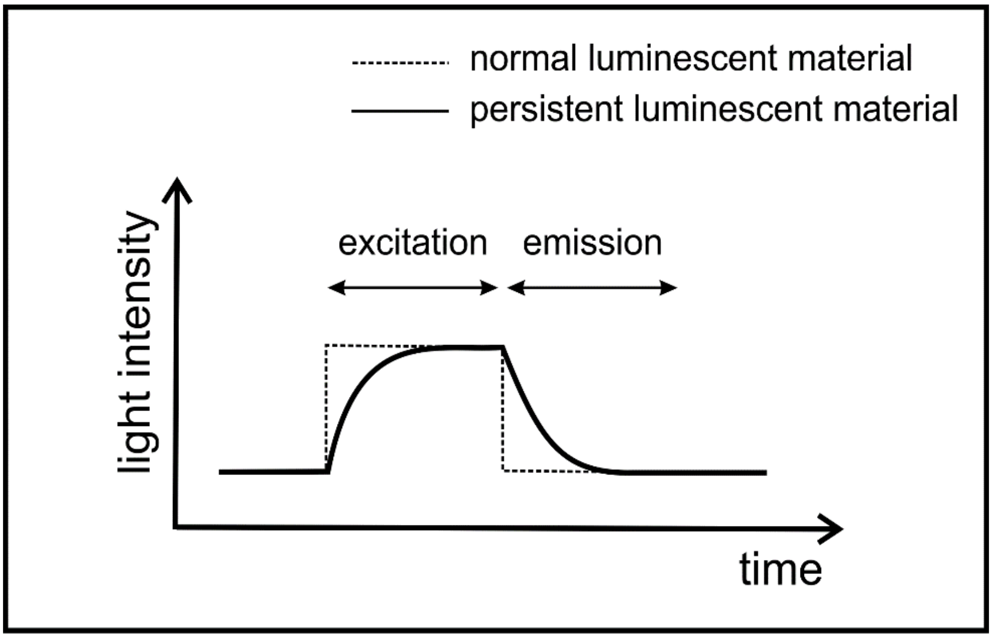

Fig. 2.4. The typical profile of luminescence involving excitation phase and afterglow phase

Usually the persistent luminescence afterglow is considered to be over when the luminiance drops under 0,32 mcd/m^2, so the afterglow time is time from the moment of termination of excitation until the luminescence luminance drops to the 0.32 mcd/m^2 [9].

2.2.2 Long lasting luminescence materials

The long lasting luminescence was an incompletely studied subject until the 1990s, although there were some luminescent materials known and used for multiple applications, such as glow in the dark watch dials and toys. For commercial applications mostly zinc sulphide with copper doping was used and, to achieve longer luminescence lifetimes and higher afterglow intensities, they were sometimes co-doped with radioactive elements [5]. The era of long lasting luminescent material research began with the discovery of $SrAl_2O_4$ doped with Eu. That was a great discovery, as the afterglow time and intensity exceeded the known compounds greatly. Not long after this discovery an improvement was made – by $SrAl_2O_4$:Eu codoping with dysprosium, the already intensive and lenghty afterglow was enhanced even more and now could reach more than 10 hours [10]. With this the study of Eu activated alkaline erath materials and other compounds began – adding different aluminates, silicates and phosphates to the list of persistent phosphors. The longest lifetime phosphors are listed in Table 2.1. They all share the same blue-green emision color, as they all contain Eu^{2+} as the luminisence center. Other emission colors are much less frequent, although there are a few materials that are non-Eu doped, but the afterglow time is significantly smaller. The overall conclusion is that the number of known compounds that exhibit a long lasting afterglow is still quite low and $SrAl_2O_4$:Eu,Dy is still one of the best persistent luminescent materials that is available, judging by the afterglow duration and intensity.

Table 2.1. Selected compounds for persistent luminescence

Material	Dopants	Peak position, nm	Afterglow duration	Source
$SrAl_2O_4$	Eu^{2+}, Dy^{3+}	520	>30h	[2]
$CaAl_2O_4$	Eu^{2+}, Nd^{3+}	440	>5h	[11]
$BaAl_2O_4$	Eu^{2+}, Dy^{3+}	500	>2h	[12]
$Sr_4Al_{14}O_{25}$	Eu^{2+}, Dy^{3+}	490	>20h	[13]
$SrAl_4O_7$	Eu^{2+}, Dy^{3+}	480	>3h	[14]
$CdSiO_3$	Sm^{3+}	400/600/650	>5	[15]
$Sr_2MgSi_2O_7$	Eu^{2+}, Dy^{3+}	470	>10h	[16]
$Sr_2P_2O_7$	Eu^{2+}, Y^{3+}	515/535	>8h	[17]
$Ba_2MgSi_2O_7$	Eu^{2+}, Dy^{3+}	505	>5h	[18]
$Ca_3MgSi_2O_8$	Eu^{2+}, Dy^{3+}	470	>5h	[19]
$Ba_3MgSi_2O_8$	Eu^{2+}, Dy^{3+}	440	>1h	[20]
Li_2SrSiO_4	Eu^{2+}, Mn^{2+}	460/535/665	>1h	[21]

The question about a white light emitting long lasting phosphor is still unresolved though. Red light emitting phosphors are not found in this list of longest afterglow phosphors that are doped with Eu^{2+} as the luminescence center. A very strong crystal field is required to lower the Eu^{2+} lowest emitting level of $4f^6$-$5d^1$ electron configuration and to produce orange or red emission [22]. Among these potential candidates, $Ca_2BO_3Cl:Eu^{2+},Dy^{3+}$ and $Sr_3SiO_5:Eu^{2+}$ are quite promising.

Theoretically speaking, white long lasting phosphors could be obtained by combination of the currently available blue, green and red phosphors. However, there is an obstacle to this idea – it is difficult to fabricate such a phosphorescent phosphor that retains the persistent white color all the time. The reason is that different phosphors seldom have very similar decay times [22].

2.3 Structural properties of $SrAl_2O_4$

A number of strontium aluminate polymorphs is known. The $SrAl_2O_4$ is a stable compund in SrO-Al_2O_3 system. It has a stable monoclinic phase at room temperature, that transforms into hexagonal when heating at temperatures above 650^o C and back to monoclinic at the same temperature during cooling. $SrAl_2O_4$ has a tridymite structure constructed by corner sharing AlO_4 tetrahedra that are tilted with respect to each other (Fig. 2.5) [23, 24]. The occupation of Al^{3+} ions in the compound leaves a charge defficiancy that is then compensated by Sr^{2+} ion incorporation in the channels created within „rings” of corner shared AlO_4 tetrahedra, therefore it is called the stuffed tridimyte structure. There are two possible positions for Sr cations in this matrix. The structure of the low-temperature phase has a three-dimensional network of corner-sharing AlO_4 tetrahedra, which has channels in the a- and c-directions where the Sr^{2+} ions are located (Fig. 2.5). The two crystallographically different sites for Sr^{2+} have different coordination numbers (i.e., 6 and 7), similar average Sr-O distances (i.e., 2.695 Å and 2.667 Å) and similar individual Sr-O distances. The two environments differ only by a slight distortion of their “square planes” [8]. When doping with Eu ions, it incorporates in the position of Sr.

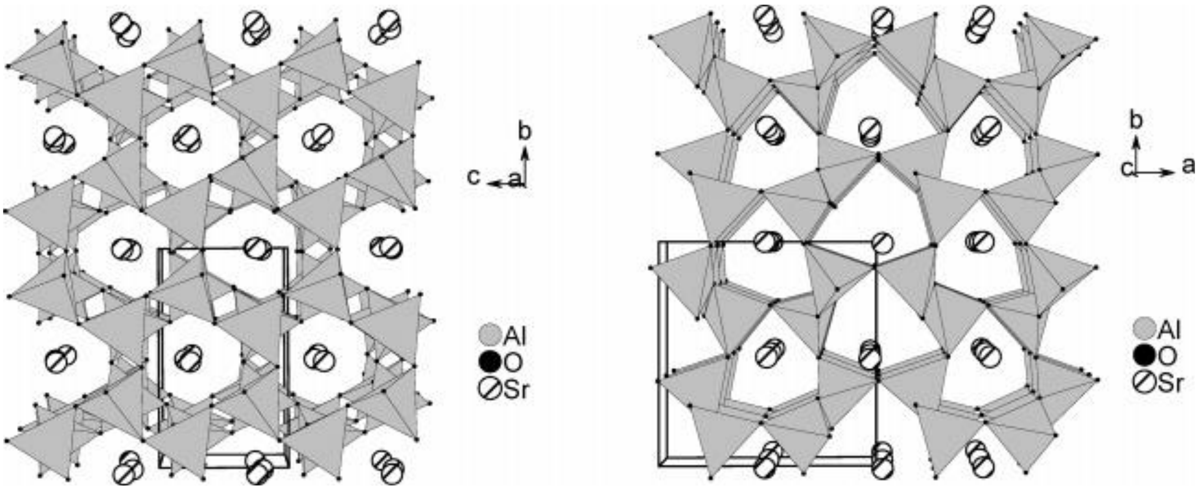

Fig. 2.5. The crystallographic structure of monoclinic phase of $SrAl_2O_4$ along the a- and c-directions. Image from [8].

The Sr^{2+} and Eu^{2+} ions are very similar in their ionic size - 1.21 and 1.20 Å, respectively and the presence of Sr(I) and Sr(II) sites results in different symmetry and orientation around incorporated Eu ion leading to deviations in the luminescent properties for both sites.

It is also important to note the dopant incorporation in the matrix, as lattice disorders and substitutional ions introduce localized states in the host matrix band gap by interrupting the long range symmetry of the material. An example of a lattice imperfection in $SrAl_2O_4$ are:

- Sr vacancy (V_{Sr}) – a point defect with 2- charge in respect to the lattice, as Sr is usually in 2+ form – thus its vacancy can be a hole trapping center itself or attract some other defect for charge compensation
- Oxygen vacancy (V_O) – a point defect with 2+ charge in respect to the lattice, as O is in 2- form thus its vacancy can be an electron trapping center itself or attract some other defect for charge compensation

There are other possibilities, like interstitial or substitutional ions, that can either be trapping centers themselves or attract other defects for charge compensation. For example – if a Dy^{3+} would replace a Sr^{2+} ion, there would be 1+ charge incompatibility. This would either act as an electron trap or these defects could cooperate – 2 Dy^{3+} ions could need 3 sites of Sr^{2+} ions. The possibility to trap an electron would also be dependent on the reduction and oxidation potential of the ion.

The dopant incorporation (Eu and Dy ions or different) in different sites of the $SrAl_2O_4$ host is usually determined by the ionic radii of the dopants and the host lattice components. From the literature it is known that the radii of the $SrAl_2O_4$ components and the dopants are as follows – see table 2.2.

Table 2.2. – ionic radii of the $SrAl_2O_4$ and the dopants

Ion	Ionic radius, Ȧ	Ion	Ionic radius, Ȧ
Eu^{2+}	1,2	Sr^{2+}	1,18
Eu^{3+}	0,95	Al^{3+}	0,53
Dy^{3+}	0,91	O^{2-}	1,4

The information given in Table 2.2 gives ground to state that Eu^{2+}, Eu^{3+} and Dy^{3+} are very likely to be found in Sr^{2+} positions. This is also confirmed by EPR measurements in [27]. If we were to consider the two possible sites of Sr^{2+}, we could estimate that they are quite similar cristallographically – therefore the dopant ions could be expected to occupy the sites more or less equally. EPR measurements confirm this statement in [27].

Also, one could note that Sr^{2+} and Eu^{2+} ions have really similar ionic radii. This can be used to explain the reason that Eu^{3+} ions incorporated in the Sr^{2+} sites of $SrAl_2O_4$ can be reduced to Eu^{2+} without any problems [8].

Clabau in article [8] reports that the formation of byproducts $Sr_3Al_2O_6$ during the synthesis of $SrAl_2O_4$ as well as the thermoluminescence measurements indicate that $SrAl_2O_4$ tends to have strontium vacancies and oxygen vacancies due to the requirement of charge neutrality. Aluminum vacancies might exist as well, but would be energetically unfavorable to form because the Al-O bonds are short and strong. Due to the requirement of charge neutrality and the absence of oxygen in the synthesis atmosphere, the codoping with Dy^{3+} should enhance the cation deficiency [8].

2.4 Luminescent properties of unactivated $SrAl_2O_4$

The band gap for unactivated $SrAl_2O_4$ is around 6.5 eV [27], therefore band to band excitation by visible light is not likely. But there are surely some defects present in the undoped material that might also be present in the material after doping. Therefore the knowledge of luminescence in undoped material could be useful in acknowledging the defects that participate in the long lasting luminescence process of the doped material. A large number of papers devoted to the investigation of long lasting luminescence of $SrAl_2O_4$:Eu,Dy do not contain any information on luminescence of undoped material as well as on nature of host intrinsic defects. Most articles do not deal with the undoped material at all. We found only several papers on luminescence of undoped $SrAl_2O_4$ and results described in these papers were contradictory. Therefore, information that can be found in literature about the luminescence of undoped $SrAl_2O_4$ is quite rare.

In some publications detectable luminescence from the undoped material under UV excitation is not reported - they mention that they have studied undoped material, but do not include any information about detecting any luminescence from it [28]. Some publications report that there is no detectable luminescence from undoped $SrAl_2O_4$ [29]. In another publication authors have detected sharp lines in the photoluminescence spectrum [30], not characteristic for intrinsic defects of a crystalline solid, the source of these lines could be trace amount of transition metals or rare earths present in the material. It is important to note that all these publications deal with luminescence at room temperature only, and emission might be different at low temperatures.

Even high purity strontium aluminates contain some amount of trace metal, that can interfere with the acquisition of correct data about intentionally unactivated $SrAl_2O_4$. However, the luminescence of trace metals in different materials is well studied and the content of trace metals in pure $SrAl_2O_4$ is less than 0.1%. The influence of trace metals luminescence in determination of pure $SrAl_2O_4$ luminescence could be negligible, however it might be detectable.

If we take a look at luminescence of undoped $SrAl_2O_4$ under different excitation sources - a broad, possibly complex, band luminescence revealing 450 and 500 nm maxima has been reported under X-ray irradiation [31], [32] that could be the luminescence of $SrAl_2O_4$ intrinsic defects, however these bands are close to those known for Eu^{2+} in this material [33]. Also, TSL of an undoped $SrAl_2O_4$ after excitation with electrons has been reported in [34], although the spectrum of the luminescence within glow peak has not been published, leaving a question – what kind of luminescence was detected and what defects might be present in the material to act as trapping and recombination centers.

To deal with these unclarities and ambiguities, the author conducted a study on the luminescence of the undoped $SrAl_2O_4$ with different excitation sources and under different temperatures.

2.5 The properties of lanthanide ions in phosphors

Lanthanide ions, either in a divalent, trivalent, or, more rarely, tetravalent state, take a very important place among luminescence centers in crystalline phosphors – both long lasting and also fast fading luminescence have wide applications, for example, the Nd^{3+} narrow line of $4f^25d$ - $4f^3$ emission in laser crystals [5], $4f^75d^1$-$4f^8$ line transition of Tb^{3+} is used as one of the components for tube lighting [5], etc. Lanthanides are commonly referred to as rare earth activators, although several of them are not very rare. There are two types of lanthanide luminescent transitions that might be of interest. Transitions between $4f^n$ levels are quite invariant in different compounds, and usually are quite sharp and line-like due to this invariance. Transitions between $4f^{n-1}5d$ and $4f^n$ configurations, however, do depend on the host matrix quite strongly, thus shifting the maximum of emission quite noticeably and also broadening the absorbtion and emission spectra [5]. The interesting properties of lanthanide ions arise from the fact that they posess a partially filled 4f shell that is shielded from the impact of crystallic field of the host by outer shell electrons.

For real life applications the color of emission as well as the quantum efficiency and the thermal stability of the process play a crucial role. All these factors are closely related to the relative and absolute location of the lanthanide energy levels [5]. For example, the position of the host-sensitive lowest 5d state relative to the host-invariant 4f states is important for the luminescence color of the obtained strontium aluminate phosphor (Fig. 2.6). The absolute position of the 4f and 5d states relative to valence band and conduction band states also affects luminescence quenching and charge-trapping phenomena [5]. For example, if we talk about the possibility of trapped charge to be thermally released from a trapping center, the energetical position of the trapping center plays a crucial role. The approach for estimation of rare earth ion levels positions in the host band scheme is presented in a number of articles by P. Dorenbos [35-38]. The main idea of this approach is that, if the positions of ground state and excited state levels are known for one rare earth ion, then the positions of these levels can be estimated in the same host for any other rare earth ion. An example of this approach use is shown in Fig. 2.6.

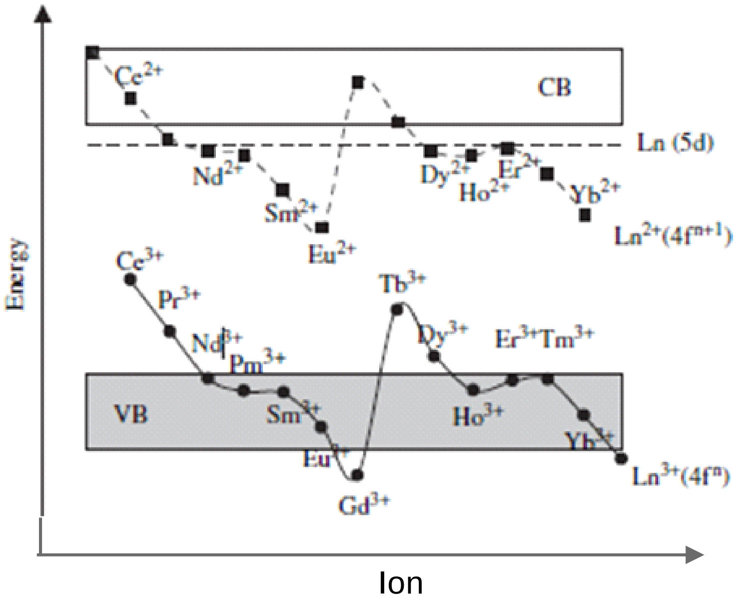

Fig. 2.6. Schematic representation of the variation of the f^n and f^{n+1} ground states of trivalent and divalent lanthanide cations in $SrAl_2O_4$. Image from [39]

As for $SrAl_2O_4$: Eu, Dy, we are looking at the case of Eu^{2+}, that acts as a luminescence center and its luminescent 5d-4f transition [35]. All the luminescent materials from aluminate and silicate groups doped with Eu show a similar emission spectrum – a broad band with the maximum within blue – green region [5]. It is quite safe to say that exactly Eu^{2+} is playing the role of luminescence center and the f-d transition is being shifted in different crystal fields while still maintaining its shape, as it can be observed in Fig. 2.7. The reasoning for this assertion is that this luminescence dissapears in samples without Eu doping, the normalized luminescence bands have almost identical full widths at half maximum – only the maximum position shifts due to differences in crystal field in different materials.

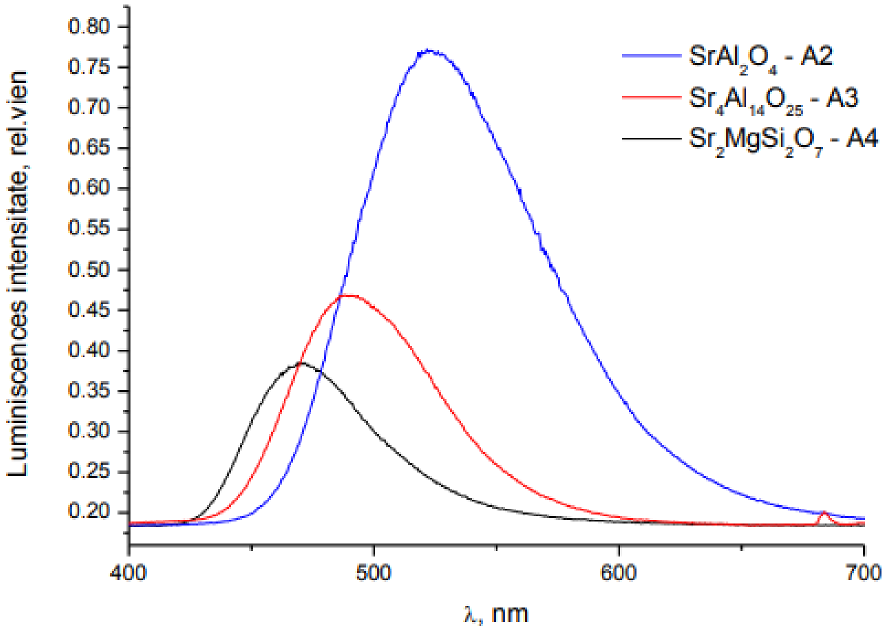

Fig. 2.7. Eu^{2+} emission in different compounds.

The co-activation of the trivalent rare earth does not change the position of the luminescence emission band nor the shape of it – for $SrAl_2O_4:Eu^{2+},RE^{3+}$ it only contributes to the afterglow time and intensity, making the duration of afterglow much longer and much more intensive. The afterglow is present also without the Dy^{3+} co-doping [40]. This is the reason we can be sure to say that the luminescence center in these compounds is Eu^{2+}, but Dy^{3+} somehow contributes to the trapping centers of the material. The photoluminescence that is characteristic to the trivalent rare earth coactivators is not observable, leading to a conclusion that direct excitation of rare earth is not involved, and nor is the energy transfer from Eu^{2+} to the trivalent rare earth.

2.5 Long lasting luminescence models

During these more than 20 years since the discovery of $SrAl_2O_4$:Eu many vast studies have been conducted to enhance the properties of long afterglow phosphors - prolong their persistent luminescence and improve the intensity. Despite this, there is still no comprehensive understanding of the mechanism of this phenomenon. This is the reason why the development of new materials and the enhancement of the properties of the known compounds is often based on trial and error methods. Different methods of synthesis have been used and studied [40]. Our research group has even tried quite exotic methods of synthesis – solar induced solid state reaction in solar reactor in CNRS-PROMES Laboratory, Odeillo-Font Romeu, France [41] and the plasma electrolytic oxidation method for long lasting luminescent coating synthesis, the paper on this result is accepted and very recently has been published [42]. The main models for long afterglow phosphors and their evolution is described in subchapters below.

2.5.1 Matsuzawa model

The search for the mechanism began with the Matsuzawa (the original patent of persistent luminescence in $SrAl_2O_4$:Eu, Dy) model [10]. In this publication the long lasting luminescence of $SrAl_2O_4$:Eu,Dy with a model where Eu^{+} ions are created during excitation is explained. Holes are then localized on Dy, that acts as a trapping center, recharging it to Dy^{4+}, and afterglow is determined by the thermal release of holes from the trapping centers and the following migration and recombination (Fig. 2.8). The essence of the mechanism lays in the presumption that an excited Eu^{2+} ion is created, a hole is delocalized from it and thus Eu^{+} is formed. The hole is trapped on Dy^{3+}, recharging it to Dy^{4+}. At a temperature that is high enough to release the trapped charges, the hole is released, migrates back to Eu^{+} and creates excited Eu^{2+}. The electron then returns to the ground state by the release of a photon. The scheme of mechanism proposed by Matsuzawa is in Fig. 2.8.

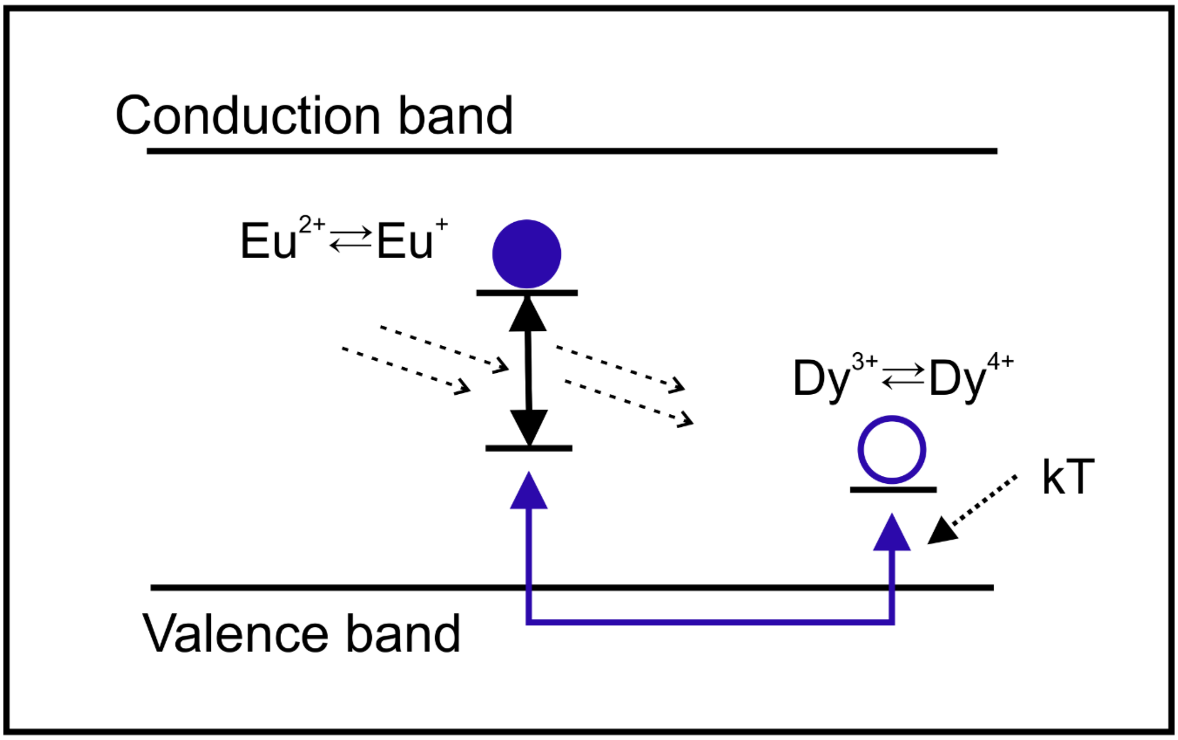

Fig. 2.8. The Matsuzawa model for the long lasting luminescence involving hole as free charge carrier

Reason for the assumption that holes are the charge carriers was photocurrent measurements [10] – under illumiation there were higher amounts of photocurrent in the vicinity of the negative electrode than in the vicinity of the positive. Matsuzawa also determined approximate trap depth – 0.65 eV.

The proposed mechanism recieved a lot of criticism – the Eu^+ state seems to be very unlikely to achieve, as high energy would be needed [43]. Also, this mechanism does not explain the afterglow of $SrAl_2O_4$:Eu without Dy co-doping. Another counter-argument for this model is that some authors claim there is no change in the charge state of the co-dopant Dy during excitation as seen from EPR and XPS measurements [44].

2.5.2 Aitasalo model

It was clear that Matsuzawa model had to be modified due to the above mentioned shortcomings. Aitasalo team consecutively proposed altogether four different possible models for the long afterglow. The first one was the least believable – a small energy photon transfers electron from valence band to a deep trapping center and another small energy photon can then transfer the electron to the excited state of this trapping center [45]. From this excited state it can then get to a shallow trapping center – oxygen vacancy. Meanwhile the hole from valence band is caught by cation vacancy. Recombination of the electron and hole occur at the anion vacancy and cation vacancy complex and the released energy is transferred to Eu^{2+}. This model would require a lot of very specific circumstances - a deep trapping center that is located energetically at the same distance from valence band as its excited state from ground state. Also a vacancy complex needs to be located in close proximity of Eu^{2+}.

The second model also involves indirect Eu^{2+} excitation [46]. Here again the electrons are promoted from valence band to some trapping centers presented in the material and the holes are trapped on the alkaline earth metal vacancy. In this model it is thermal energy that helps to release the electron from the trapping center and it migrates to an oxygen vacancy. The energy that is released in the recombination process is then transfered to Eu^{2+} ion and it becomes excited. This process is followed by Eu^{2+} trasition to ground state and the characteristic light is emitted. The scheme of this mechanism is in Fig. 2.9.

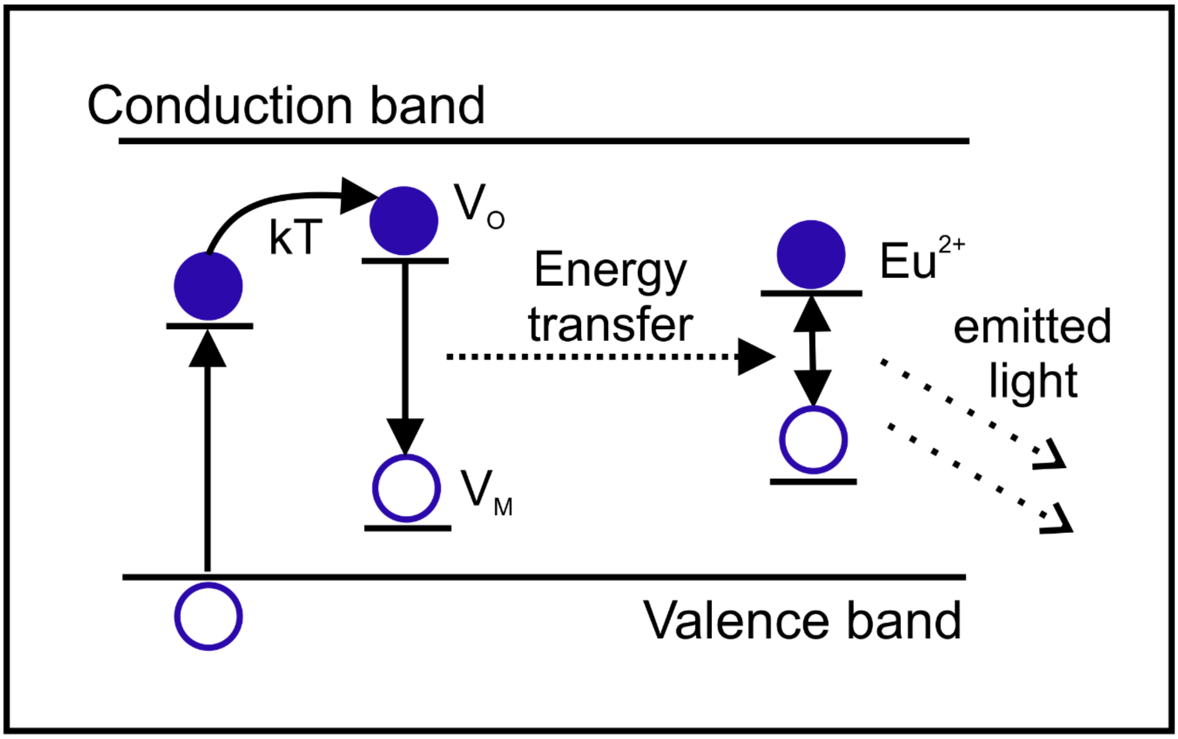

Fig. 2.9. The Aitasalo model for the long lasting luminescence involving indirect Eu^{2+} excitation

The energy transfer and oxygen and alkaline earth metal ion vacancy complexes play a crucial role in this mechanism. Also, the luminescence center needs to be in close proximity to the vacancy complex for an efficient energy transfer process. In this mechanism it was assumed that under excitation the holes in valence band are created. These holes are considered to be the only free charge carriers. Therefore the proposed mechanism excluded formation of Eu^+ and propose the possibile migration of electrons between somewhat different traps. However it is not clear what the defects could be, for electron traps having the energy levels below to that of oxygen vacancy. This mechanism is good in the way that it does not limit the role of co-dopants to be charge trapping centers. Aitasalo proposed that trivalent rare earth co-doping could possibly be responsible for larger number of lattice defects – due to the charge compensation.

As for the incompatibilities of this model – different articles have discussed the location of 5d-levels for Eu^{2+} and they seem to be located just below the conduction band. This would indicate the electron to be the free charge carrier rather than the hole.

Later on Aitasalo proposed corrections on his previous work, presenting a different model [47]. As the previous models for mechanism of long lasting luminescence [45,46] recieved quite a lot of criticism on the physical accuracy, additional experiments were conducted to clarify the actual role of the co-dopants. The TSL of Dy co-doped and non co-doped materials was studied and led to a conclusion, that co-doping does not alter the position of thermoluminescence peak [47]. Thus one must come to the conclusion that Dy does not act as the trapping center and the process could be more complex. Therefore Aitasalo modified the model proposed by Dorenbos [35] involving some details. The proposed processes are as follows - electron is thermally promoted from Eu^{2+} excited state to the conduction band, electron migrates through the conduction band and can then be localized on defects – oxygen vacancies as well as trivalent rare earth ions. The scheme of this model is in Fig. 2.10.

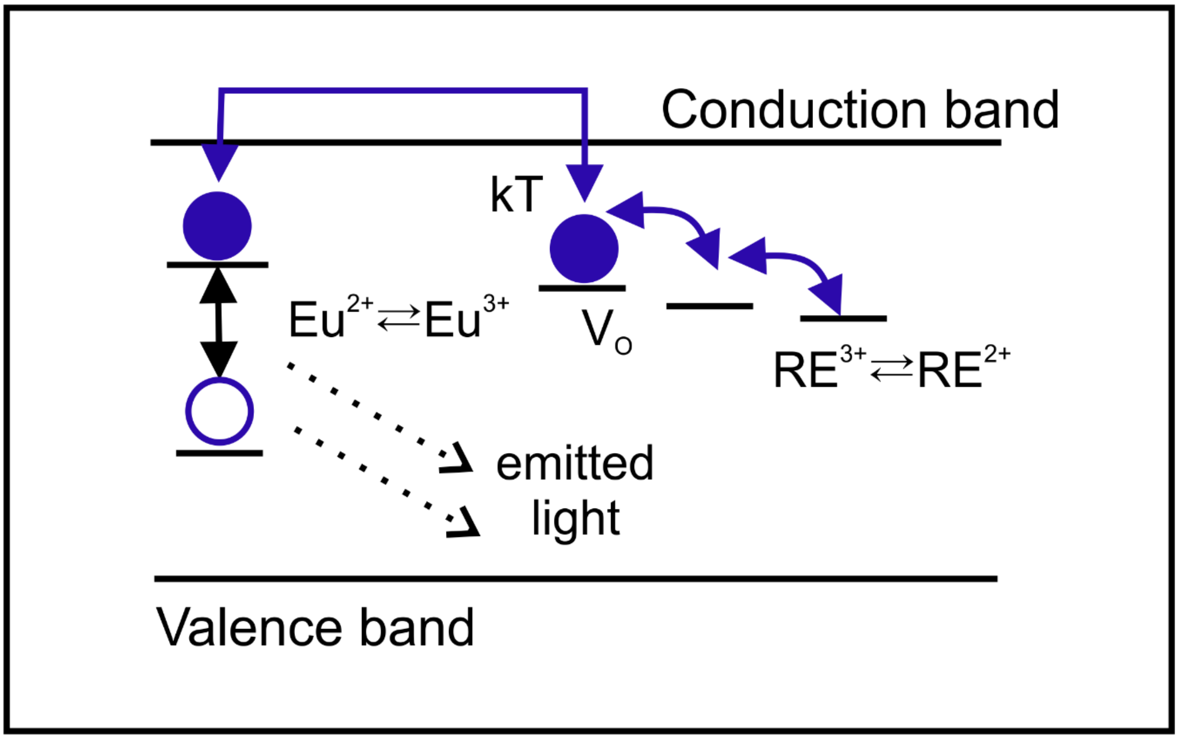

Fig. 2.10. The model proposed by Aitasalo for the long lasting luminescence involving Eu^{3+} accumulation during excitation

Charge carriers can also migrate from one trap to another and finally migrate back to the luminescence center, where excited Eu^{2+} transition to ground state creates the characteristic luminescence.

The fourth work [48] on the topic of mechanism of persistent luminescence presented a very similar idea to that described in [47], that was also verified by XANES and EXAFS measurements that confirm Eu^{3+} accumulation during excitation. However, when explaining the mechanism, Aitasalo emphasizes that there are doubts about Eu^{3+} presence, but Eu^{2+} and hole complexes might be more believable and the recombination of these complexes with electron is the source of the long lasting luminescence. The main difference from previous model and that proposed by Dorenbos [35] is involvement of several kinds of electron traps.

2.5.3 Clabau model

Clabau suggested a model that involves electrons as the free charge carriers. To present proof for this hypothesis, electron paramagnetic resonanse experiments were conducted. The experimental results showed that the concentration of Eu^{2+} ions changes during excitation and afterglow – it decreases in the excitation phase and increases during afterglow [49]. Therefore Clabau presumed Eu^{2+} could be ionized - after Eu^{2+} excited state is formed during UV irradiation. Electron migration from trapping centers to the luminescence centers in this model does not happen through the conduction band, but with the aid of a direct transition between traps, that can occur if the levels are located in close proximity to each other.

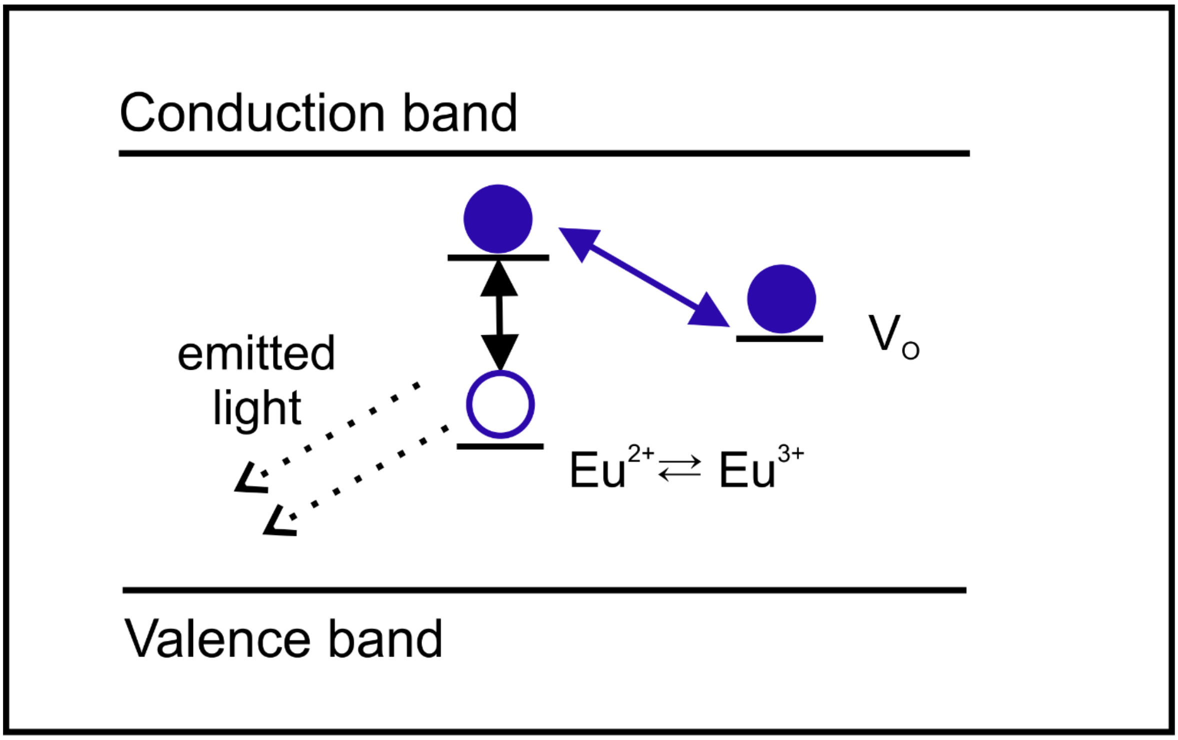

Fig. 2.11. Clabau model for the long lasting luminiscence involving direct electron transition from luminescence center to trapping center.

This model was based on the photoconductivity measurements in different temperatures – no increase of photoconductivity is observed at 300 K, whereas at this temperature trapped charges are being released from trapping centers. In this model there is a different approach to Dy role in the material – it is not regarded as a charge carrier trapping center, but as a stabilizing element for the oxygen vacancies – the presence of Dy^{3+} ions could modify electron density to an oxygen vacancy [49]. In this model oxygen vacancies are considered to be the electron trapping centers.

It is not actually clear, how Dy^{3+} could stabilize oxygen vacancies, because when Dy^{3+} replaces Sr^{2+} an uncompensated positive charge remains. This charge compensation could be achieved by creation of Sr vacancies. Therefore the hypothetical process where Dy^{3+} could be stabilising the creation of oxygen vacancies should be quite complicated. There are no experiments to be found in literature that validate this assumption.

2.5.4 Dorenbos model

The study of excitation and luminescence processes of $SrAl_2O_4$:Eu,Dy completed by Dorenbos led to the new version of long lasting luminescence mechanism [35].

Dorenbos presented the locations of the Eu^{2+} d-bands in the band gap of $SrAl_2O_4$ matrix. The estimation of positions of dopant energy levels in $SrAl_2O_4$ material is discussed in [38]. The Eu^{2+} energy levels are located right beneath the bottom of the conduction band and Dy^{2+} level is located around 0.9 eV below the conduction band. This information is consistent with the TSL measurements. In this model electron is thermally promoted from Eu^{2+} excited state to the conduction band, as the energy difference is small and therefore thermal ionization at room temperature is very probable. The electron migrates through the conduction band and is trapped by Dy^{3+} thus recharging it to Dy^{2+}. Electron can be thermally released from Dy^{2+} and can contribute to forming the Eu^{2+} excited state via two possible ways – either it is again thermally excited to the conduction band or it can transition to the ground state with photon emission (Fig 2.12).

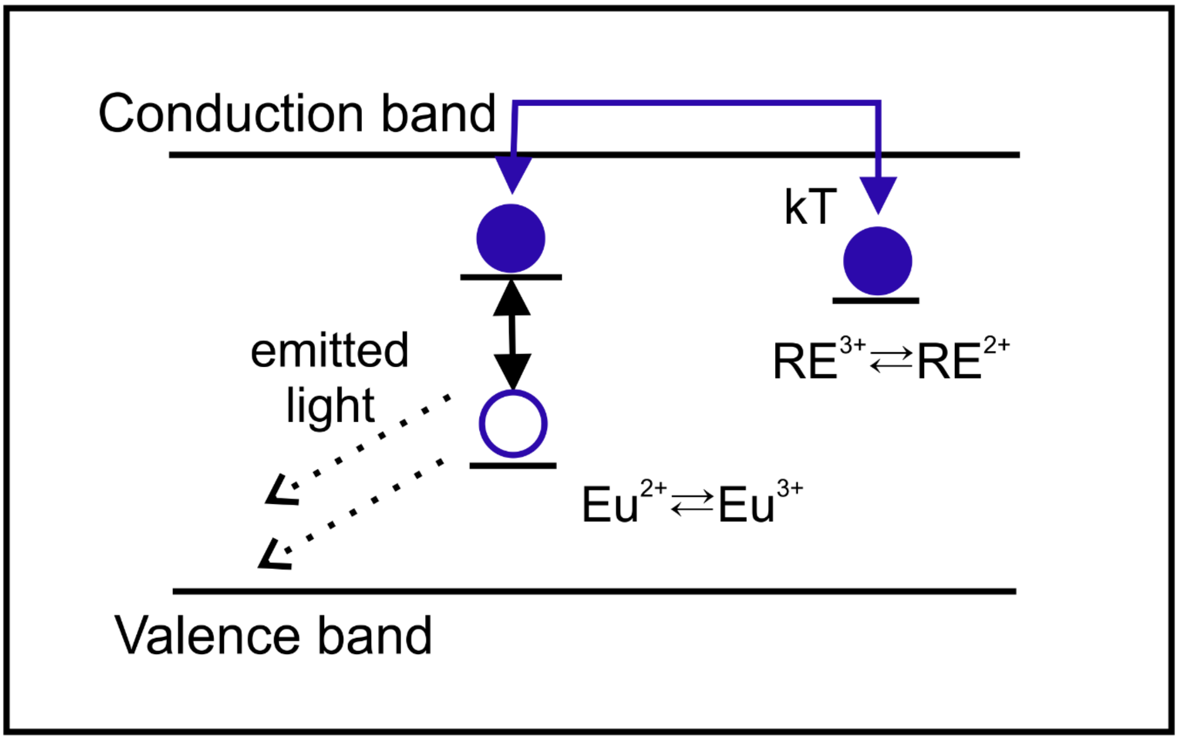

Fig. 2.12. Dorenbos model for the long lasting luminniscence involving electron migration through conduction band

2.5.5 Holsa model

Holsa turned attention to the results of XANES measurements of $SrAl_2O_4$:Eu,Dy [50] and tried to observe any valence changes of dopandts in the material during excitation and emission. He concluded that under excitation only the Eu^{2+}/Eu^{3+} oxidation happens, therefore some changes to the known models are proposed. There is an assumption that in $SrAl_2O_4$:Eu,Dy UV radiation leads to the excitation of Eu^{2+}. The host matrix conduction band is close to the excited Eu^{2+} level therefore some electrons can escape from the excited levels of Eu^{2+} by the help of surrounding thermal energy to the conduction band. Clabau [49] and Dorenbos [35] similarly have stated that electron from Eu^{2+} excited state is thermally transferred to conduction band. The electrons migrate through the conduction band and are eventually trapped on a defect level. The trivalent rare earth co-dopants can also act as electron traps. Thermal energy can then liberate the charge carriers from the trapping centers and they can either be de-trapped or return to luminescence center.

Although Holsa did his last part of research not on $SrAl_2O_4:Eu^{2+},Dy^{3+}$, but on the $Sr_2MgSi_2O_7:Eu^{2+},RE^{3+}$ material, it is presumed that the mechanism might be quite similar in both long lasting luminophores. The defects, that are claimed to be present in this material, are cation vacancies, oxygen vacancies and interstitial ions as well as the dopant ions. The cation vacancies can be created due to the evaporation of alkali earth metal oxide during the high temperature solid state reactions. Cation vacancies were involved also due to the charge compensation when a trivalent rare earth ion replaces divalent ion site in the host matrix while oxygen vacancies may be created due to the reducing atmosphere during material preparation. The introduction of oxygen and strontium vacancies as well as the Eu^{2+} ion creates electron traps essential for the persistent luminescence [50].

All of these long afterglow mechanisms involve the generation of migrating charge carriers during excitation that are localized in trapping centers afterwards. The cause of persistent afterglow is thermally stimulated gradual charge release from trapping centers with resultant recombination. The differences in these models concern (I) charge carriers – electrons or holes; (II) the charge carrier migration – does it happen through valence, conduction band or levels of trapping centers; (III) the excitation of luminescence - does the charge carrier directly transfers to the luminescence center or the luminescence center is excited with the aid of energy transfer process; (IV) the nature of trapping centers – intrinsic defects or co-activator.

The analysis of the results that are described in these publications show, that the most appropriate model for the explanation of $SrAl_2O_4$:Eu,Dy material is as follows: during excitation Eu^{3+} centers are created and electrons are localized in trapping centers. After the release of electrons from trapping centers they recombine with Eu^{3+}, creating excited Eu^{2+} and a radiative Eu^{2+} transition to ground state is the cause of luminescence.

There are some shortcomings in the above described model – does the electron recombination with Eu^{3+} occur only by thermal release of electrons from trapping centers; there is no evidence if the charge state change of co-activator Dy^{3+} can or can not take place; as well as there is hardly any data about intrinsic luminescence of $SrAl_2O_4$ that could allow the identification of intrinsic defects.

3. Methodology

3.1 Sample synthesis

The persistent luminescence properties of a material are strongly affected by the synthesis, because, as stated beforehand, different impurities are responsible in some way for the luminescence mechanism and the incorporation of different defects is influenced by the method of synthesis [5, 22]. Also, phosphorescent properties are influenced not only by the defects, but also by the crystallite size – and that can also be varied by the means of different synthesis [22]. Therefore below is a short overview of the most common ways of $SrAl_2O_4$:Eu,Dy sample synthesis as can be found in literature.

3.1.1 Solid state method

Solid state method is the most common method for the syntesis of Eu doped long lasting phosphors. The reason for this is that it is the most simple way to prepare solid compounds. It consists of heating two or more nonvolatile solids together in order to produce the required product. The method is commonly used in both industry and the laboratory, and considered to be one of the best way in synthesizing oxide materials [22]. For the preparation of $SrAl_2O_4$:Eu,Dy, the stoichiometric amounts of $SrCO_3$, Al_2O_3, $Eu(NO_3)_3$ and $Dy(NO_3)_3$ powders are mixed together and heated in a furnace in reducing atmosphere (for example, 5%H2, 95%N2) and temperature as high as 1300°C. The reduction of the Eu^{3+} in this method happens starting from 1250°C. The obtained powder properties such as the crystallite size and admixture of other aluminate phases does depend strongly on the rates of heating and cooling therefore it is quite difficult to obtain a single phase [51].

3.1.2 Chemical precipitation

Chemical precipitation is a formation of a separable solid substance from a solution, either by changing the substance into an insoluble form or by changing the composition of the solvent to reduce the solubility of the substance in it. For the preparation of $SrAl_2O_4$:Eu,Dy, $Al(NO_3)_3$, $Sr(NO_3)_2$, $(NH_4)_2CO_3$, $Eu(NO_3)_3$ and $Dy(NO_3)_3$, are used as starting materials. The starting materials have to be dissolved in distilled water to obtain the solutions of the necessary molar concentration and stirred together to form a homogeneous solution, and the

$(NH_4)_2CO_3$ solution is dropwise added to form precipitates. then the obtained precursor has to be washed with water and ethanol. After drying, the precursor has to be calcinated in reducing atmosphere at the minimum temperature of 1250° C. This results in the monoclinic $SrAl_2O_4$ phase with the typical crystallite size of around 70 nm, showing an increase in the crystal size with the increase in calcination temperature [52].

3.1.3 Sol – gel method

Sol- gel method is a widely employed wet method to prepare materials. It is the conversion of starting materials into a colloidal solution (sol) acting as the precursor for an integrated network (gel) of discrete particles. Sol-gel method can be classified into two routes – aqueous sol-gel and nonaqeous sol-gel method depending on the nature of the solvent utilized. [53]. For the preparation of $SrAl_2O_4$:Eu,Dy, the compounds $Al(NO_3)_3$, $(NH4)_2CO_3$, $Sr(NO_3)_2$, $Eu(NO_3)_3$ and $Dy(NO_3)_3$, are used as starting materials. The beginning of the process is roughly the same as in chemical precipitation method until a polymerizing agent is added (for example, PEG 600) and a gel is formed. The obtained gel must then be heated to remove water. The resultant precursor powder is afterwards heated at different temperatures for sufficient long time to form $SrAl_2O_4$:Eu,Dy powder. The phase transition to monoclinic-hexagonal crystal structure of $SrAl_2O_4$ occurs at around 650°C – therefore this method has an advantage of a lower temperature for phosphor preparation as compared to other methods [22, 53].

These are the more common methods for the synthesis of the $SrAl_2O_4$ material. There are other less common methods described in literature, such as:

- CO_2 laser vaporization
- Solvothermal precipitation
- Solar induced solid state synthesis
- Microemulsion
- Hydrothermal synthesis

and other methods.

Table 3.1 contains information for general comparision of long lasting luminescence materials synthesized by different methods.

As for the concentrations of the dopants, a question arises considering the best concentrations of dopants that should be added to achieve the most intensive and longest duration afterglow.

Table 3.1. The comparison of commonly used techniques for long lasting phosphor synthesis

Synthesis method	Particle size	Homogeneity	Synthesis temperature (º C)	Afterglow duration	Reference
Solid state reaction	Micrometer scale	Bad	>1250	Long	[51]
Sol-gel	Nano to micrometer scale	Medium	600-800	Medium	[53]
Chemical precipitation	Nano to micrometer scale	Good	>1000	Short	[52]
Hydrothermal synthesis	Nano to micrometer scale	Good	>1000	Short	[54]
Combustion	Nano to micrometer scale	Medium	>1000	Short	[55]

There are numerous articles where 1% and 1 or 2 % are referred to as the optimal concentration of dopant and codopant, though it is not by any means verified. Most authors choose to follow these typical concentrations of 1% Eu^{2+} and 1 or 2% Dy^{3+}. Lin et al. claims the ideal ratio of Dy/Eu ions to be 2/1 in $Sr_4A_{l4}O_{25}$ [56], and Jiang et al. found the optimal luminescent properties in $Ca_2MgSi_2O_7$:Eu^{2+},Dy^{3+},Nd^{3+} at a Dy/Eu ratio of around 20/7 [57].

In all cases europium comes as the starting product in the reaction mixture in its oxidized state Eu^{3+} (Eu_2O_3, $Eu(NO_3)_3$), and observable phosphorescence of Eu^{2+} appears after a reducing treatment. In a number of articles it is stated - luminescence measurements show that after this reducing treatment, europium is mostly present in the reduced form Eu^{2+}, but Mossbauer measurements reveal that there around 5 to 10% of Eu^{3+} remain as residue. XANES measurements show that the codopant dysprosium does not change its charge state and after the excitation is swiched off Dy is present in its stable form Dy^{3+} [8].

In the current study samples prepared by the sol-gel method are used.

3.2 X-ray diffraction

The X-ray diffraction method (XRD) is a material characterization technique. This method can give useful knowledge about the phase composition of the crystalline material as well as some information about the crystallite size and unit cell dimensions. The method uses filtered, monochromatic X-rays from a cathode ray tube that interact with the periodic structure of the crystal lattice of the sample.

Usually the obtained X-ray diffraction pattern is compared with data from data bases, for example, InternationalCenter for Diffraction Data (ICDD) Inorganic Crystal Structure Database [00-034-0379].

In the present study the PANalytical X'Pert Pro diffractometer was used for structure determaination of the syhthesized materials as well as the determination of crystallite sizes. This diffractometer is equipped with X-ray tube with Cu anode, operating at cathode voltage of 45 kV and current of 40 mA , producing Cu Kα radiation (1.5418 Å).

For the crystallite size estimation Rietveld method was used, that considers both the full width at half maximum (FWHM) of the diffraction pattern as well as the instrumental circumstances of the measurement.

3.3 Luminescence measurements

For luminescence measurements at differrent temperatures two kinds of cryostats were used – liquid nitrogen cooled cryostat (working temperatures 90-450 K) and closed cycle helium cryostat (working temperature 9-300 K). For temperatures above room temperature a sample holder with heater was used. For all cases Lakeshore temperature controller was used for precise temperature logging and controlling.

The luminescence spectra as well as the luminescence kinetics and the TSL measurements were recorded with Andor Shamrock B303-I spectrograph (spectral resolution ~1nm) that is equipped with a CCD camera (Andor DU- 401A-BV) at the exit port. A simplified equipment scheme is in Fig. 3.1.

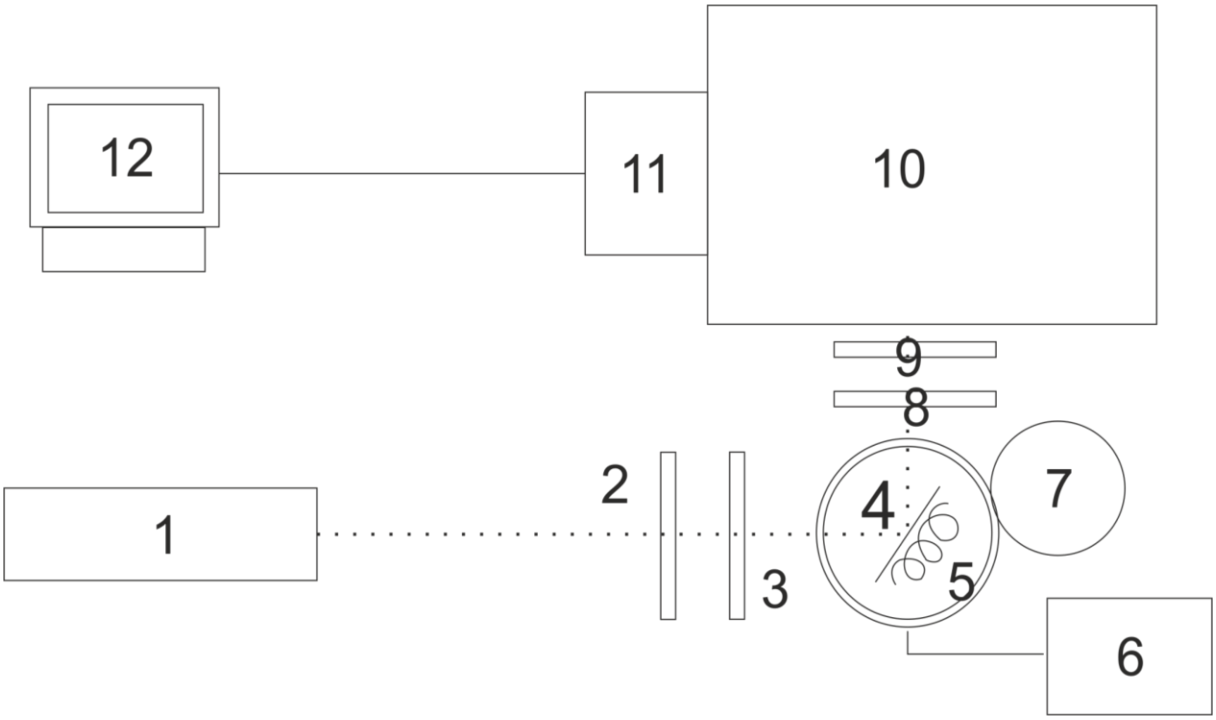

Fig. 3.1. Simplified scheme of equipment for luminescence measurements

1. Excitation source
2. Filter
3. Fused quartz window
4. Cryostat and sample holder
5. Heater
6. Temperature controller
7. X-ray tube
8. Fused quartz window
9. Filter
10. Spectrometer
11. CCD camera
12. Computer

The scheme for experiments was slightly modified from the one in Fig 3.1 using different sources of excitation:

1. X- ray source (W anode, 45 kV, up to 10 mA)
2. Diode pumped YAG:Nd laser LCS-DTL-382QT (266 nm, 8 ns) for photoluminescence excitation

3. Laser with variable wavelength (OPO) NT342/3UV (EXPLA) – for measurements of excitation spectra

The total measurement error is estimated below 10%, which is mainly due to the geometry of equipment - a slight change in the geometry of the measurement and the intensity of the recorded luminescence also changes. Diffraction grating of the spectrometer can shift and must be callibrated manually, as well as the intensity of the YAG:Nd laser changes in the range of 5%.

One must note that we are dealing with relative intensities when talking about luminescence spectra, because even slight changes in the positioning of the sample will give different results in light intensity. When recording the spectra of the samples and repeatedly putting the sample in and taking out of the sample holder, the registered intensities of the spectra do not change more than 5%, if the configuraton is preserved. What can be said for sure is that the intensity profile remains unchanged during one measurement – that is, the form of the spectrum is correct and we can normalize it and compare it to a normalized spectrum from another measurement.

3.4 Luminescence time dependence

Luminescence decay kinetics in the case of intrinsic luminescence follow the rules of a monomolecular reaction. It can be described with a first order equation

$$-\frac{dn}{dt} = \alpha n \tag{1.}$$

where n – number of the involved centers. By integration, we get

$$-\int_{n_0}^{n} \frac{dn}{n} = \alpha \int_0^t dt \tag{2.}$$

$$n = n_0 e^{-\alpha t} \tag{3.}$$

By definition $I \sim \frac{dn}{dt}$ and I = γ dn/dt, therefore

$$I = \gamma \alpha n_0 e^{-\alpha t} \tag{4}$$

at t = 0 the I=I_0 and thus $I_0 = \gamma \alpha n_0$

And taking note, that lifetime τ is inversely proportional to the probability of transition α, we obtain:

$$I = I_0 \exp\left(-\frac{t}{\tau}\right) \tag{5.}$$

That clearly shows that this kind of luminescence decay can be described with a single exponential function.

In the case of recombination the decay kinetics can obey the laws of bimolecular reaction and can be described by a hyperbolic function (6.). Solving the corresponding differential equations in an equivalent manner as in the first we can obtain

$$-\frac{dn}{dt} = \beta n^2 \tag{6.}$$

The solution of the equation for the luminescence intensity is:

$$I = \frac{I_0}{\left(1+(I_0\beta)^{\frac{1}{2}}t\right)^2} \tag{7.}$$

Where I – luminescences intensity, I_0 – the initial intensity after termination of excitation at t = 0, ß– transition probability, t – time.

There are other possibilities for describing kinetics as well – for example, in the case of disorder around the luminescence center, one can get a stretched exponential function [58]. In case of tunneling luminescence, the luminescence decay of excited states created in tunnel processes depends on spatial distribution of defects involved and can often be described with the empirical Bequerels law, that for longer t values can be expressed like this [59]:

$$I(t) \sim t^{-1} \tag{8.}$$

Equation (5.) describes the kinetics of luminescence decay, if the decay is determined by the lifetime of the luminescence center excited state. There are two possibilities – the luminescence kinetics can be determined either by the excited state life time or by the time for creation of excited states. In first case the creation time for the luminescence center excited state is shorter than the excited state life time, for example, direct excitation of the luminescence center with short excitation pulse. In the second case the creation of excited luminescence center can be a more complicated process, that involves energy and/or charge transfer. In this case the life time of the luminescence center excited state can be shorter than the time that is necessary for the transfer processes and the luminescence intensity dependence on time is determined by transfer processes.

If the luminescence kinetics are determined by the excited state life time of the luminescence center, the luminiscence is usually short – the decay time is within nanosecond range for allowed transitions and not exceeding several miliseconds for partially forbiden transitions. In long lasting luminescence materials the luminescence decay kinetics depend on the charge carrier release from trapping centers, and that, however, depends on the energetical depth of the charge carrier trapping centers, temperature of the sample and charge migration.

A good example is Eu^{2+} that has an excited state life time of 10^{-6} s [5], therefore without the presence of other defects, it can not provide the long lasting afterglow, but the long afterglow, that was observed in different Eu^{2+} activated materials takes place due to gradual delocalization of charge carriers from some kind of trapping centers.

3.5 Thermally stimulated luminescence

Thermally stimulated luminescence (TSL) or thermoluminescence is the emission of light from a material due to the release of trapped charge carriers during heating of the material provided it has previously accumulated energy during excitation by trapping charge carriers. This phenomenon is used as a material characterization technique that is based on excitation of a material at relatively low temperature (but sometimes also at room temperature) and the recording of glow peaks while heating the material. The method is more informative if luminescence spectra are recorded within glow peaks. The glow peak position and shape can be used to obtain useful information about the trap levels in the material. TSL was first mathematically described by Randall and Wilkins, also establishing the connection between the shape of a TSL curve and the parameters of a system [60].

The basic concepts underlying TSL process are related to those of phosphorescence. There must be some intrinsic defects or impurities in the host material within its forbidden gap, that can form discrete energy levels (donor/acceptor levels), some of them being also luminescence centers. A number of these lattice structural defects and impurities provide unoccupied energy levels, that are called trapping centers due to their capability to localize charge carriers before they recombine on the luminescence center. These traps can be either electron or hole traps, depending on what charge carriers localize on them. The energy that is necessary for charge carriers to be released from the trapping centers is referred to as “trap depth”, also known as thermal activation energy.

From the configurational coordinate model and the model of electron in a potential well one can understand that the probability of electron release from a given trap level at that particular temperature, is

$$p = \frac{1}{\tau} = s \exp\left(-\frac{E}{kT}\right) \tag{9}$$

where s is the frequency factor, k is the Boltzmann constant, τ is the time electron spends on the trap, E is the activation energy and T is the absolute temperature. The release of electrons from trapping centers depends exponentially on the absolute temperature. In practice linear heating rate is used after the termination of irradiation. For a given trap there will be an increase of charge carrier release intensity, followed by a decrease, when the population of the trap starts to decrease. Plotting the luminescence intensity as a function of temperature will give a single glow peak or multiple glow peaks, depending on the number of trap levels.

The simplest model of glow peak analysis (10.) involves a first order process - a single type of electron trap with activation energy E and concentration n and a single type of radiative recombination center and a negligible probability of retrapping [60]. In this case the luminescence intensity will be

$$I \sim -\frac{dn}{dt} = s\,n\exp\left(-\frac{E}{kT}\right) \tag{10.}$$

where s is the frequency factor, k is the Boltzmann constant, τ is the time electron spends on the trap, E is the activation energy and T is the absolute temperature. The formula can be adapted for a second order equation [60]:

$$I \sim -\frac{dn}{dt} = s'n^2\exp\left(-\frac{E}{kT}\right) \tag{11.}$$

or generalized for higher order processes that involve complex multi-defect systems.

The methods for peak analysis range from very simple empirical ones to more sophisticated methods.

An overview of the commonly used methods for determining the depth of trapping centers can be found in Table 3.2. Equation 13. has been used for trap depth determination in the current study.

Table 3.2. Commonly used methods for determining the depth of trapping centers in TSL

Equation	Reference	Equation Nr.
$E\ (eV) = T_{max}(K)/500$	[61]	(12.)
$E = \frac{2kT_{max}^2}{\delta}$	[61]	(13.)
$\frac{\beta E}{kT_m^2} = s * \exp\left(-\frac{E}{kT_m}\right)$	[60]	(14.)
$\frac{E}{k}\left(\frac{1}{T_{m1}} - \frac{1}{T_{m2}}\right) = \ln\left(\frac{\beta_1}{\beta_2} * \frac{T_{m2}^2}{T_{m1}^2}\right)$	[60]	(15.)

E – activation energy, “trap depth”
k – Boltzmann constant
β – heating rate
T_m – maximum temperature of glow curve
s – frequency factor
δ – the full width at half maximum

4. Results and discussion

4.1 Synthesis of samples

Three different kinds of samples were prepared for this work – $SrAl_2O_4$ doped with Eu and Dy; $SrAl_2O_4$ doped with Dy and the undoped $SrAl_2O_4$ samples. All these samples were prepared using the sol-gel method.

Strontium nitrate ($Sr(NO_3)_2$, purity 98%, Sigma Aldrich), aluminum nitrate nonahydrate ($Al(NO_3)_3 \cdot 9H_2O$, purity 99,6 %, VWR Prolabo Chemicals) were used as the starting materials for $SrAl_2O_4$. Urea (NH_2CONH_2, purity 99,5 %, Sigma Aldrich) was used as a chelating and a gelling agent. These chemicals were used without any further purification.

$Eu_2(NO_3)_3$ and $Dy(NO_3)_3$ were used for activators and were mixed with the precursor powders in order to obtain 1 mol% Eu and 1 mol% Dy concentration in the samples. The appropriate amount of $Sr(NO_3)_2$ and $Al(NO_3)_3 \cdot 9H_2O$ were dissolved in deionized water. After the $Sr(NO_3)_2$ and the $Al(NO_3)_3 \cdot 9H_2O$ were dissolved completely, an appropriate amount of urea was added to the solution (the molar ratio of all metals ions and urea was 1:20, respectively). Also, an appropriate amount of deionized water was added so the molar concentration of all metals ions in the solution would be 0.2 M. Then this mixture was heated at 90 °C until white gel was formed. When the gel consistency was obtained, then this gel was heated at 400 °C in an open oven for 2 hours for nitric oxides elimination and the white powder was obtained. After synthesis, the obtained sample was calcined at 1200 °C for 2 hours in a reductive atmosphere and white powders were obtained [62].

The structure of all our strontium aluminate samples before and after the reducing heat treatment was characterized by X-ray powder diffraction.

For the size estimation of the crystallites, the Rietveld method was used, that considers both the full width at half maximum (FWHM) of the diffraction pattern as well as the instrumental circumstances of the measurement. The estimated crystalline size from the XRD data was 30–50 nm.

The analysis of obtained XRD patterns of $SrAl_2O_4$ powder (Fig.4.1) and the comparison of these XRD patterns with data from International Centre for Diffraction Data (ICDD) Inorganic Crystal Structure Database [00-034-0379] confirms the dominant phase of all the samples is monoclinic $SrAl_2O_4$, and content of other phases, if present, is under 10%. In some samples traces of $SrAl_4O_7$ was present. The XRD patterns of the $SrAl_2O_4$, $SrAl_2O_4$:Eu,Dy, and $SrAl_2O_4$:Dy samples are in Fig 4.1 a), b), and c).

Therefore it is expected that processes responsible for luminescence of synthesized material can be mainly governed by $SrAl_2O_4$ monoclinic phase in undoped and doped samples.

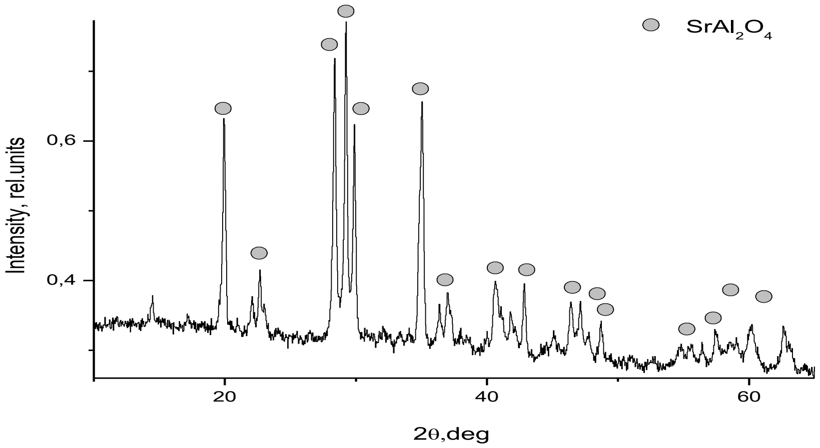

a) The X – ray diffraction pattern of undoped $SrAl_2O_4$ sample

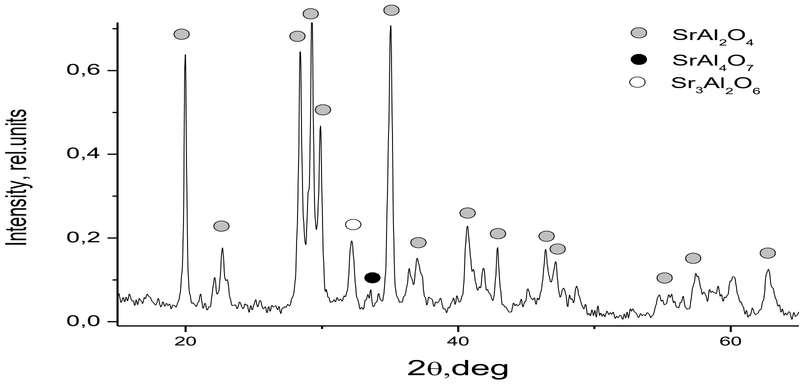

b) XRD pattern of $SrAl_2O_4$:Eu,Dy sample

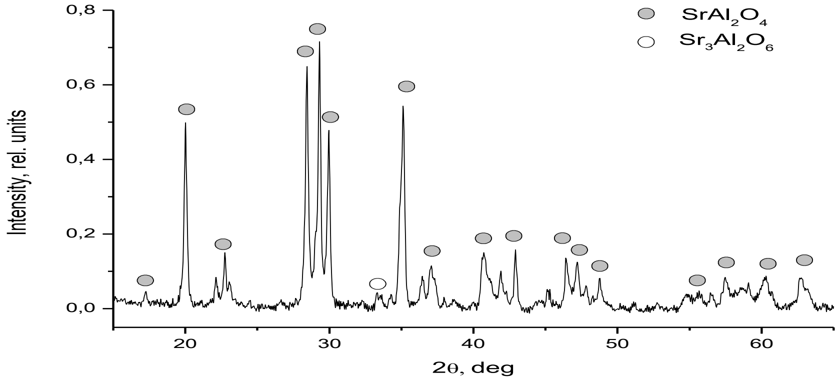

c) XRD pattern of $SrAl_2O_4$:Dy sample.

Fig. 4.1. The X – ray diffraction patterns of undoped and doped $SrAl_2O_4$ samples

4.2 Luminescence of $SrAl_2O_4$:Eu,Dy

The photoluminescence spectrum of SrAl2O4:Eu,Dy sample at room temperature was recorded (Fig. 4.2). The afterglow of SrAl2O4:Eu,Dy is a broad band with maximum at 529 nm. The peak position and shape is in agreement with those observed by other researchers for SrAl2O4:Eu,Dy [40], thus the luminescence observed is mainly from SrAl2O4:Eu,Dy monoclinic phase and possible contribution from other phase is negligible. The luminescence center for this emission is Eu2+ and it emerges from the 5f - 4d allowed radiative transition as stated in [5]. The green persistent luminescence afterglow of this sample can be observed for time exceeding 10 h.

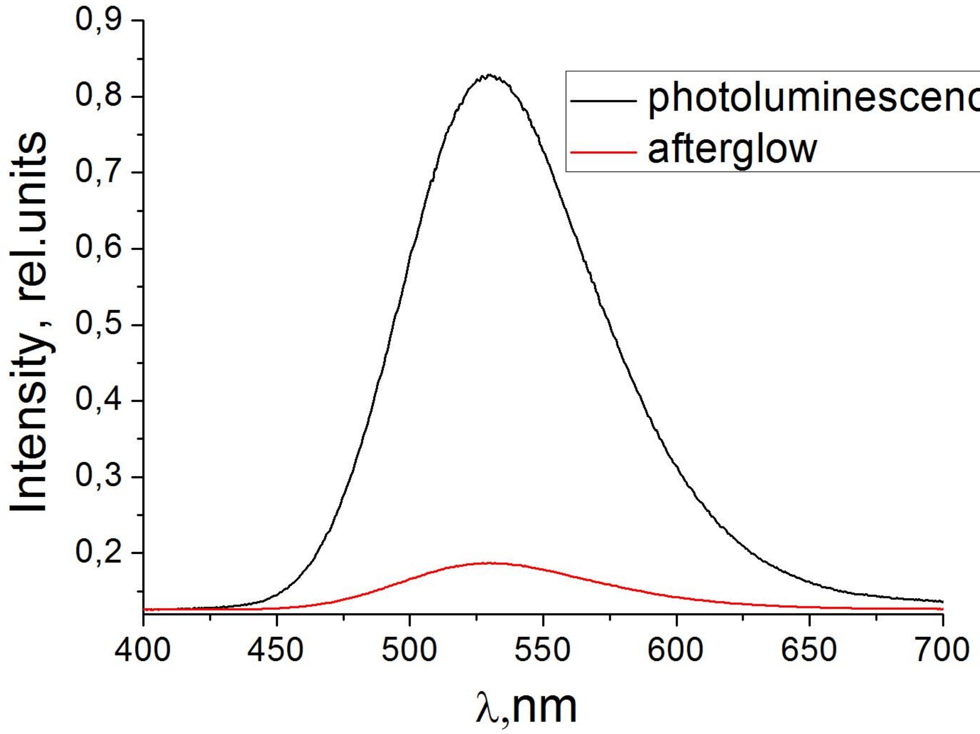

Fig. 4.2. Long lasting luminescence of $SrAl_2O_4$:Eu,Dy at RT, photoluminescence (266 nm excitation) and afterglow spectrum.

After that the sample was cooled down to low temperatures using nitrogen cryostat for a measurement of TSL. What was observed was quite surprising – the luminescence afterglow intensity when cooling down the sample was still large enough to be clearly detectable. That leads to a discussion – if only thermally stimulated processes take place in the sample to ensure the persistent luminescence – could there possibly be enough thermal energy at 90 K temperature for the de-trapping process of charge carriers? That most definitely seemed like a matter worth looking into.

To begin dealing with the above mentioned question, the long lasting luminescence for $SrAl_2O_4$:Eu,Dy was excited at three different temperatures – at RT (~295 K), 240 K and 90 K and the afterglow was observed at each of these temperatures. The corresponding afterglow emission spectra were recorded and are presented in Figure 4.3. When lowering the temperature of excitation, we can observe that the intensity of afterglow luminescence decreases relative to the intensity of afterglow luminescence excited at room temperature, afterglow luminescence excited at 90 K is reduced three times.

To compare the spectral distribution, all the afterglow spectra were normalized – it is visible that the peaks at different temperatures coincide well (inset in Figure 4.3.) - this means that the maximum position and shapes of emission bands are almost the same for all three excitation temperatures. Therefore it can be stated that the luminescence center as well as its surroundings are the same at room temperature, 240 K and 90 K.

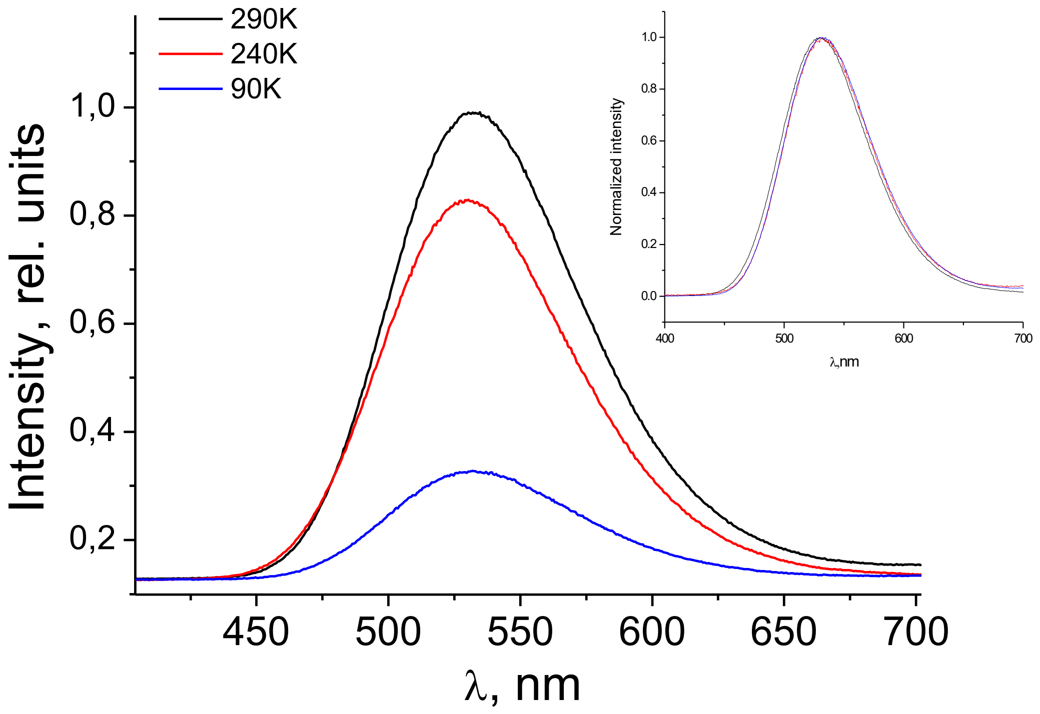

Fig. 4.3. Luminescence afterglow spectra at different temperatures (266 nm excitation). Inset – normalized luminescence spectra coincide.

The probability of thermal release of charge carriers - electrons and holes in $SrAl_2O_4$:Eu,Dy might be negligible at 90 K, as was already discussed before. This statement needed some proof. Therefore, in order to check the possible contribution of thermally stimulated processes in the afterglow, the sample was excited with X-rays to fill in traps at 10 K for 20 minutes, then heated up (2 K/min) while recording the emission spectra where, after processing the obtained data, thermally stimulated glow curve was acquired at the maximum of emission. The acquired glow curve in Figure 4.4. shows two overlapping glow maxima within 200 – 400 K and a less intense peak at around 135 K, below that temperature there are no evident peaks, meaning no thermal release of electrons. (Fig. 4.4.) .

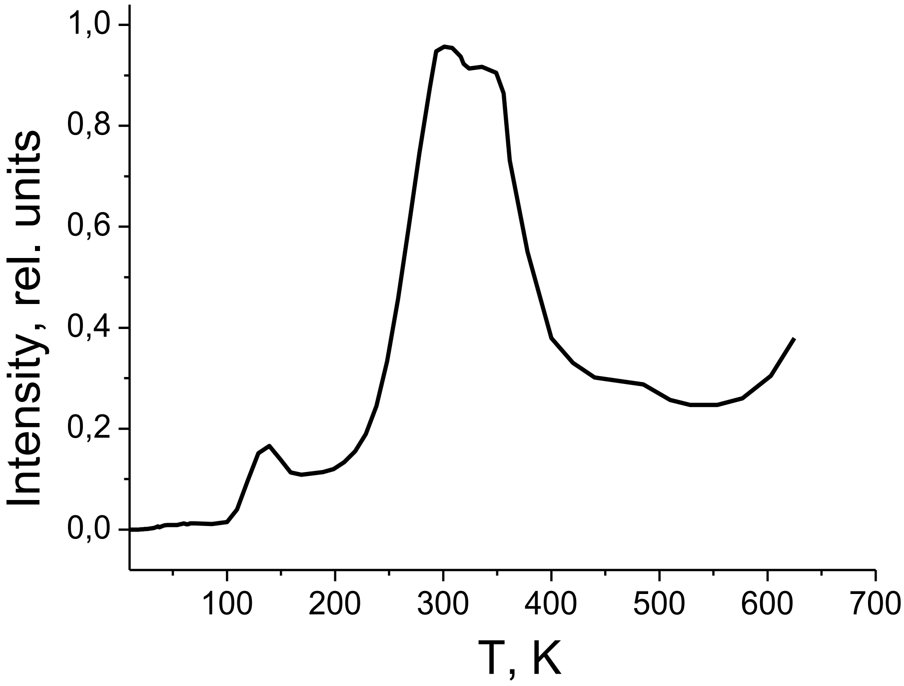

Fig. 4.4. Thermally stimulated luminescence glow curve of $SrAl_2O_4$:Eu,Dy

The luminescence spectra within glow peaks are the same as recorded for afterglow, indicating the luminescence center is Eu^{2+}.

The TSL glow curve is quite similar to those that appear in several publications, for example [63]. The two intense maxima indicate two kinds of charge carrier traps with a slight shift in activation energies for charge release relative one to another. The activation energies were roughly estimated for the two larger maxima (these are the maxima that are responsible for the charge release around RT) using the empirical equation (13.) from Table 3.2. The estimated activation energies were around 0.52 eV and 0.59 eV. These activation energies are close to those described in [40]. The activation energy was estimated to be approximately 0.27 eV for glow maxima at 135 K. Thus we can assume that the long afterglow detected for

$SrAl_2O_4$:Eu,Dy sample excited at 90 K is not due to thermally released charges recombination on luminescence center [64] - the electrons and holes in $SrAl_2O_4$:Eu,Dy at 90 K are localized at traps and do not have enough thermal energy to be released from them. Therefore it can be concluded that one of the processes that is involved in the long afterglow mechanism is electron tunneling from trap to the Eu^{3+} thus creating the excited Eu^{2+}. The important condition for electron tunneling is that the electron wave functions must overlap for electron initial and final state.

Based on the results of TSL measurements and the emission spectra the author puts forward a hypothesis - in the formation of excited Eu^{2+} luminescence center both processes are involved – 1) thermally released electron migration through conduction band that, possibly after multiple trapping-detrapping processes, returns to Eu^{3+}, creating excited Eu^{2+} center, as well as 2) electron tunneling to Eu^{3+} from closely located trapping centers, thus creating excited Eu^{2+} center also. The ratio of the contribution of these processes to the whole afterglow mechanism is temperature dependent. The study of long lasting luminescence dependence on excitation temperature [65] showed that in $SrAl_2O_4$:Eu,Dy the electron traps in proximity of Eu are probably deeper than those well separated spatially. If the electron trapping center that is associated with Eu^{3+} is slightly deeper than others, the electron life time at this trap must be longer than at shallower traps and thus it is possible that even at room temperature the last step of the process could be electron tunneling to Eu^{3+} from trapping center that is located in close proximity to the luminescence center.

The tunneling luminescence might be observed because of three possibilities:

1) During excitation both holes and electrons are trapped in close proximity to the luminescence center and they successively tunnel to Eu^{2+}, creating the excited state and the transition to ground state happens with emission of a photon.
2) The second possibility involves the creation of an excited state formed by a hole tunneling to Eu^{+}. In this process Eu^{2+} excited state is formed, and the transition to ground state happens with emission of a photon.
3) Luminescence center Eu^{2+} is ionized during excitation, creating Eu^{3+}. Electron from trapping center tunnels to Eu^{3+}, thus Eu^{2+} excited state is formed, and the transition to ground state happens with emission of a photon.

The analysis of these processes leads to a conclusion that the first two possibilities are less probable. In the first one it is necessary for two kinds of trapping centers to be in close proximity to Eu^{2+} - both hole and electron trapping centers. The formation of many three-particle complexes like that is not very likely.

The second possibility involves the creation of excited state formation by hole tunneling to Eu^{+}. But, as already stated in the literature review, for an excited Eu^{2+} one electron is in 5d state, while Eu^{+} ground state has $4f^6$ electrons and the 5d states are unoccupied. Therefore, the hole tunneling to Eu^{+} means that the 4f state is depleted and the creation of excited Eu^{2+} center is problematic.

The third option involves Eu^{3+} creation during excitation process and excited Eu^{2+} center creation by electron tunneling to Eu^{3+} from the trapping center. Eu^{3+} luminescence has not been observed in afterglow spectra. However, when exciting $SrAl_2O_4$:Eu,Dy luminescence at low temperatures with X-rays, there are sharp lines in 570-590 nm region, that might be attributed to Eu^{3+} luminescence or Dy^{3+} luminescence (the origin of these lines is discussed in paragraphs 4.3 and 4.4). This seems the most likely option, moreover in article [44] the XANES spectrum is measured for $SrAl_2O_4$:Eu,Dy and the changes in intensity have been tracked, observing that there is a relative increase in the peak area of the Eu^{3+} ions of about 4% during irradiation. This would confirm the creation of Eu^{3+} takes place during irradiation and thus support the third possibility.

The luminescence intensity dependence on time for excited luminescence centers created in tunnel processes depends on spatial distribution of defects involved and can often be described with the empirical Becquerels law (8). This is defined by the spatial distribution of the defects involved. Therefore, the decay kinetics could give additional evidence to confirm the presence of tunneling processes in the material. For this a measurement of luminescence decay kinetics was conducted.

The luminescence decay of $SrAl_2O_4$: Eu,Dy excited at 90 K temperature can be seen in Fig. 4.5.

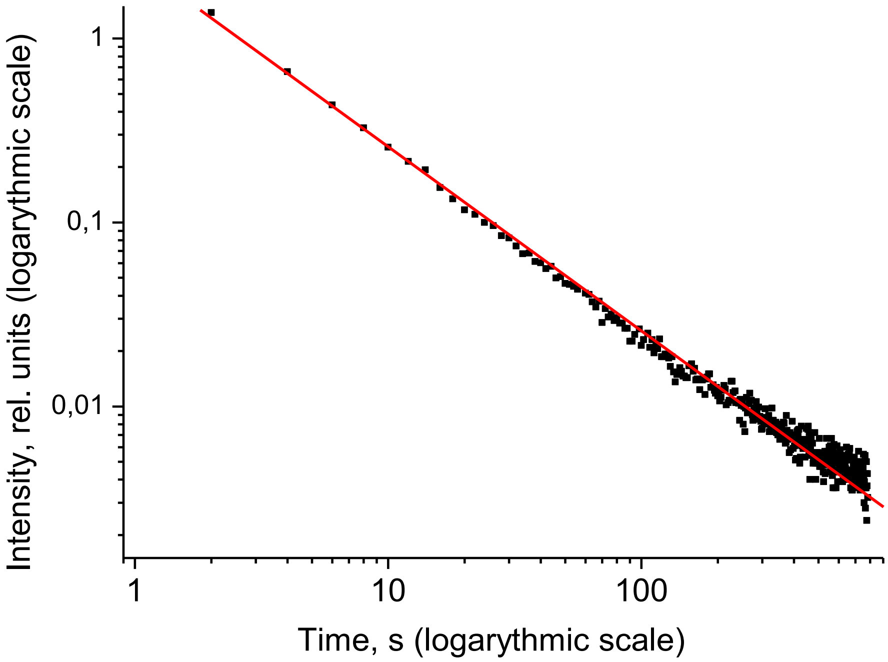

Fig. 4.5. The decay kinetics of $SrAl_2O_4$:Eu,Dy luminescence afterglow excited with X-Ray at 90 K in logarithmic scale

The plot of intensity as a function of time in logarithmic scale is well approximated by a straight line with the slope of approximately 1 – this result goes together well with the Becquerels law. This therefore can be considered as additional evidence to support that at 90 K the Eu^{2+} excited state formation occurs via electron tunneling. Since the tunneling of electron is temperature independent process, it can take place also at a higher temperature. This process can be similar to that described by Kotomin et al. for diffusion controlled tunneling [59]. However, further study and data analysis is necessary to confirm simultaneously active thermally stimulated and tunneling processes in $SrAl_2O_4$:Eu,Dy.

All the above mentioned evidence leads us to suggesting some improvements to the long afterglow mechanism models that are available in the publications. We suggest that the charge carriers are electrons and at low temperature, e.g. 90 K, the electron tunneling is dominant process in creation of excited Eu^{2+} center. In turn, at high enough temperature the electrons are released from traps. The thermally released electron during migration can be re-trapped and released multiple times. The last step of electron migration could be either its direct trapping at Eu^{2+} excited state or trapping at deeper trap associated with Eu^{3+} that is followed by eccited Eu^{2+} center creation via tunneling. The radiative decay of Eu^{2+} excited states created via both processes is the origin of observed luminescence. The scheme of proposed mechanism is in Fig. 4.6. The mechanism described is simplified since the glow curve gives strong evidence that two electron traps were and spatial distribution between Eu^{3+} and its associated electron trap could be Therefore another study and analysis according to the description set out in [66,67] could be benefitial for obtaining additional information on simultaneously active thermally stimulated and tunneling processes in $SrAl_2O_4$:Eu,Dy [64].

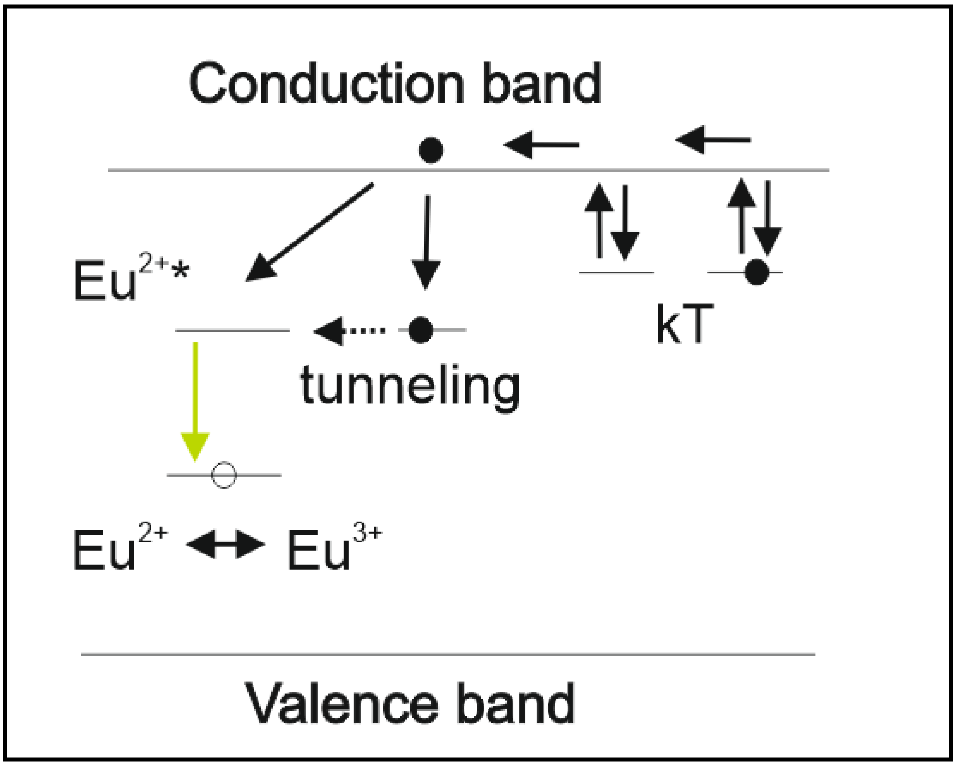

Fig. 4.6. The possible model for persistent luminescence in $SrAl_2O_4$:Eu,Dy

This discovery is actually of major importance towards the applicability of persistent luminophores in outdoor situations. In Fig. 4.7. can see the usual ambient air temperatures in Latvia as well as the TSL glow curve for a commercial $SrAl_2O_4$: Eu, Dy sample.

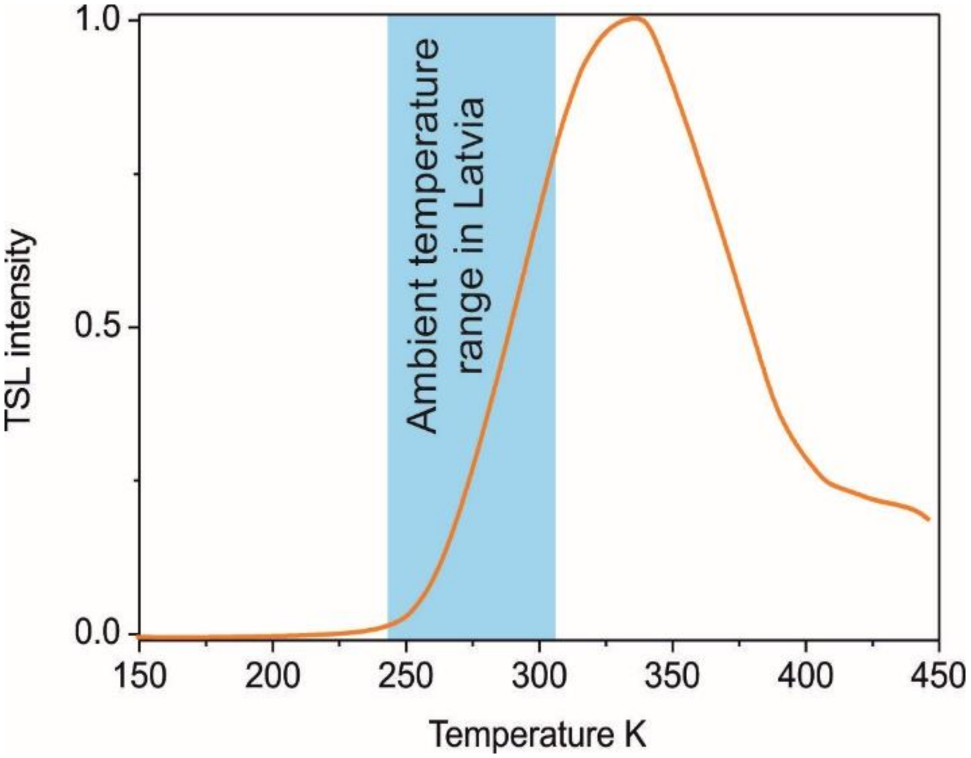

Fig. 4.7. TSL glow curve for a commercial $SrAl_2O_4$:Eu,Dy sample and the ambient air temperature range in Latvia

As it is well observable in Fig. 4.7., the ambient air temperatures in Latvia can make this luminophore lose over 90% of its intensity in coldest times. And that is a major drawback for the possible outdoor applications, for example, glowing roadsigns that do not work in winter would not be something that anybody would be interested in. Therefore – if it was possible to improve the ratio of temperature independent tunneling luminescence process versus the thermally stimulated process, that could improve the situation greatly.

4.3 Low temperature studies of $SrAl_2O_4$:Eu,Dy

All of the experimental results, that were discussed in 4.3 led to the conclusion, that the low temperature studies of $SrAl_2O_4$:Eu,Dy might result in new knowledge of the persistent luminescence mechanism in this material. A large number of researches of persistent phosphors have been conducted for temperature range around room temperature and above due to the possible applications of material. The studies of luminescence processes in $SrAl_2O_4$:Eu,Dy at low temperatures are not frequently found in publications as the afterglow is weak or not observed below 240 K after photoexcitation [68], and mainly photoluminescence is investigated, turning less attention to X-ray excited afterglow [68].

Therefore the attention was turned to the studies of low temperature luminescence in $SrAl_2O_4$:Eu,Dy material.

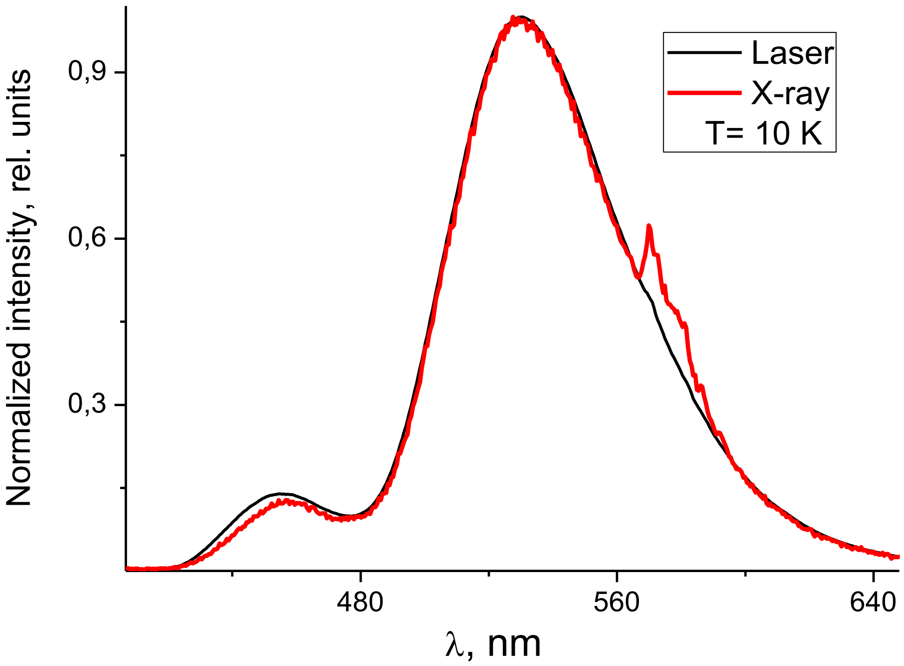

Fig. 4.8. Photoluminescence (266 nm) and X-ray excited $SrAl_2O_4$:Eu,Dy luminescence spectra at 10 K temperature

First, the emission spectrum of $SrAl_2O_4$:Eu,Dy at 10 K under X-Ray excitation was recorded (Fig. 4.8.) and compared to the photoluminescence spectrum under 266 nm excitation at 10 K. These two spectra reveal some interesting information – not one, but two luminescence bands peaking at 450 nm and 520 nm can be observed in luminescence spectrum of $SrAl_2O_4$:Eu,Dy at low temperatures under excitation; the 450 nm band undergoes thermal quenching at temperatures above 150 K. The afterglow of 450 nm luminescence is with a considerably shorter lifetime at low temperatures – only about a second, explaining the fact, that it is not visible in the afterglow spectra recorded several seconds after the termination of excitation. Various ideas concerning the origin of the 450 nm luminescence band have been expressed in literature [49,68,69]. The role of Eu^{2+} ions was discussed within these ideas. The most probable explanation for the appearance of this second luminescence band is that the Sr ion in $SrAl_2O_4$ can incorporate in two slightly different positions, and, as Eu^{2+} incorporates instead of a Sr ion, the energy of radiative transitions for both sites is not the same, it could therefore be shifted energetically to each other.

The luminescence spectra of X-ray excited $SrAl_2O_4$:Eu,Dy reveals additional luminescence peaks overlapping with Eu^{2+} band. Literature study reveals that these additional bands could possibly be attributed to Dy^{3+} luminescence or Eu^{3+} luminescence. The three Dy^{3+} luminescence bands are mentioned in [44], whereas one Dy^{3+} band is mentioned in [70,71]. Dy^{3+} and Eu^{3+} ions have emission peaks in relatively close positions, therefore additional experiment is needed to confirm the origin of these lines.

4.4 Luminescence of $SrAl_2O_4$:Dy

The author carried out the study of strontium aluminate doped only with Dy to confirm the origin of emission line groups in $SrAl_2O_4$:Eu,Dy. The emission spectrum of $SrAl_2O_4$:Dy sample under X-ray excitation can be seen in Fig. 4.9.

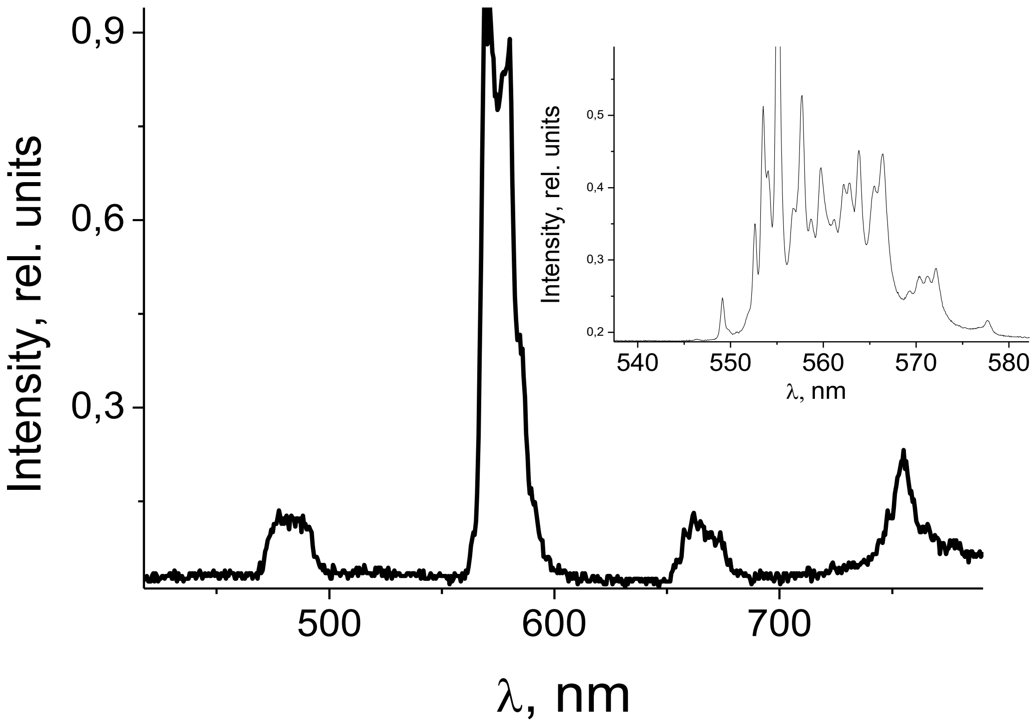

Fig. 4.9. Luminescence spectrum under X-ray excitation of $SrAl_2O_4$:Dy sample at 10 K

There are four luminescence bands centered at ~ 483 nm, 576 nm 664 nm and 754 nm. The positions of these emission bands coincide well to the maxima described in [70,72]. However, the shapes of emission bands are quite different from those described in [70], where the luminescence bands are simple, but according to our results the emission band shape reveals a possible contribution from multiple closely located and partially overlapping lines. These lines are barely resolved at room temperature, therefore the spectrum was recorded at 10 K. The spectrum for more intense band at ~ 576 nm in higher resolution is shown in inset in Fig. 4.9., and it reveals a group of emission lines. Since the interaction of Dy^{3+} with host matrix is weak [73] the luminescence spectra of Dy^{3+} ion should be similar in a number of materials and the spectrum can be compared with luminescence of Dy^{3+} in YAG:Dy [73] and $GdAlO_3$:Dy [74]. In these spectra, the sets of overlapping Dy^{3+} emission lines are in regions 460 – 500 nm, 550 – 610 nm as well as a low intensity band at 677 nm and this is very close to that observed in our experiment; the shapes of bands are similar to those recorded in our experiment. Based on that, one must conclude that the $SrAl_2O_4$:Dy under X-ray excitation exhibits dominantly Dy^{3+} luminescence. The comparison of luminescence spectra of $SrAl_2O_4$:Eu,Dy (Fig. 4.8.) and $SrAl_2O_4$:Dy (Fig. 4.9.) reveals that in luminescence spectrum of $SrAl_2O_4$:Eu,Dy the position of lines within 568 – 600 nm exactly matches the position of more intense lines in luminescence spectrum of $SrAl_2O_4$:Dy. Therefore it is shown that under X-ray excitation in $SrAl_2O_4$:Eu,Dy both – dopant Eu^{2+} and co-dopant Dy^{3+} are excited and contribute in luminescence spectrum.

It is worth noting the intensity of Dy^{3+} luminescence at RT is more than twice of that at 10 K (Fig. 4.10.), indicating that at 10 K only a fraction of X-ray generated electrons and holes undergoes recombination at Dy^{3+}. It can be assumed, that the other fraction of charge carriers are trapped at defects, for confirmation the measurements of TSL were conducted.

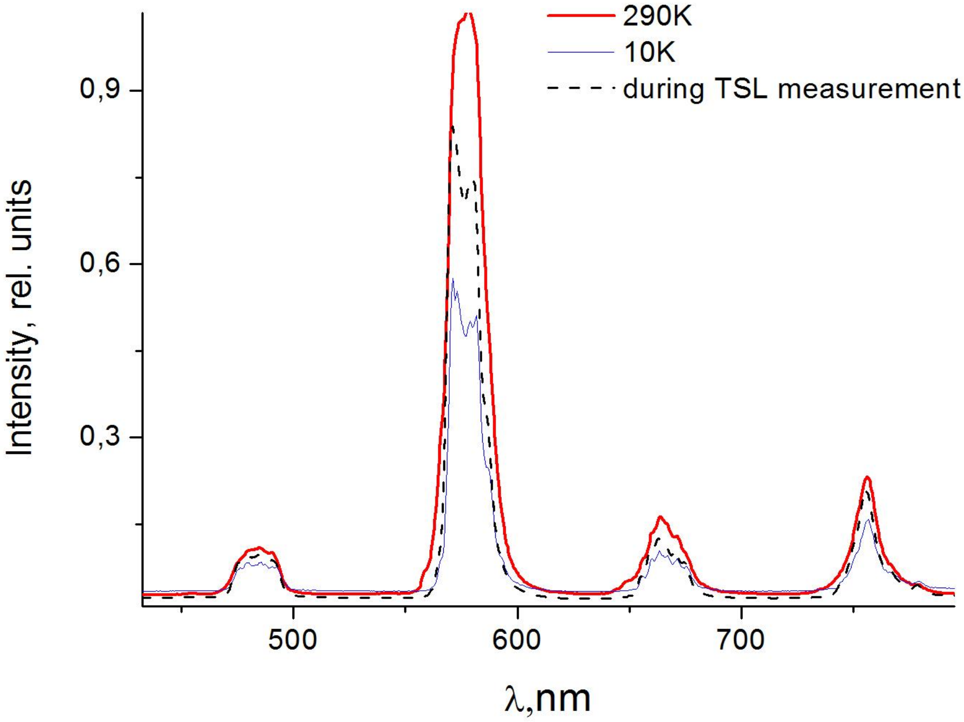

Fig. 4.10. Emission spectra of $SrAl_2O_4$:Dy under X-ray excitation at 10 K and room temperature and the spectrum during TSL measurement

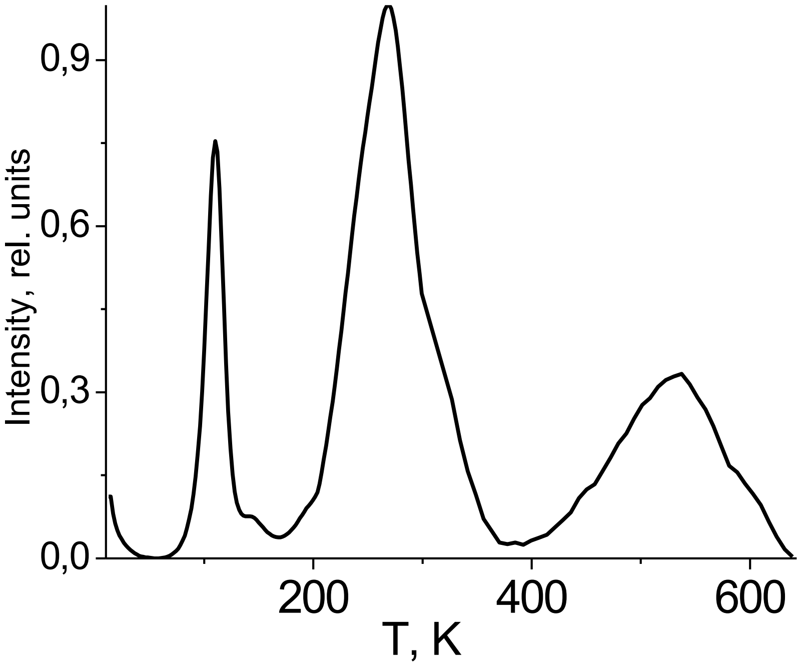

Fig. 4.11. X-ray induced TSL of $SrAl_2O_4$:Dy sample.

The sample was excited by X ray at 10 K for 20 minutes. TSL glow curve of $SrAl_2O_4$:Dy is presented in Fig. 4.11. and three major glow peaks are observed at 110 K, 270 K and 532 K. The luminescence spectra in all the glow peaks coincide with the emission spectrum under X-ray excitation at 10 K (Fig. 4.9.), meaning that only Dy^{3+} luminescence bands were observed in TSL without the contribution from any other luminescence. There is one more thing in the TSL glow curve that requires clarification - the low temperature part of the measurement shows gradual decrease in the glow intensity within 10 – 60K. The origin of this decrease might be a glow peak at very low temperature or creation of excited Dy^{3+} from another descending source. Therefore the time dependences of luminescence intensity decrease at 10 K during time interval necessary for sample heating from 10 K to 50 K and during temperature rise within 10 – 50 K were recorded. The luminescence intensity decay coincide well for both experiments – the TSL measurement in Fig. 4.11. and kinetics measurement in Fig. 4.12. proving, that the initial intensity decrease at the low temperature part is due to afterglow, not a TSL peak and this excludes the thermostimulated process. This is evidence that there is not an additional TSL maximum in the low temperature range. Therefore, one can assume there are no wery shallow traps, which release charges within the temperature range 10-60 K [75]. It is important to point out the absence of glow peaks in the very low temperature range. Thus the origin of the afterglow recorded at 10 K is due to the creation of excited Dy^{3+} luminescence centers via electron tunneling. Similar afterglow revealing Eu^{2+} luminescence is observed for $SrAl_2O_4$:Eu,Dy at 10 K, indicating the same tunneling process takes place.

The thermally stimulated glow curves, if we compare the $SrAl_2O_4$:Eu,Dy and $SrAl_2O_4$:Dy sample, are different one from another, as expected, but some things are worth noting (see Fig. 4.4. and Fig. 4.11.). The TSL peak at the region 100-150K was observed in $SrAl_2O_4$:Dy as well as in undoped $SrAl_2O_4$, therefore it could possibly be attributed to intrinsic defects.

It is generally accepted that during afterglow the excited Eu^{2+} center is created via Eu^{3+} recombination with electron [49,68]. Therefore, the glow peaks correspond to the thermal release of electrons from traps and the excited Dy^{3+} centers can appear in TSL measurement due to Dy^{4+} recombination with electrons. The electrons were trapped at host defects; possibly at oxygen in distorted tetrahedra of AlO_4 [76]. These terahedrons could be distorted by the rare earth ions and this distortion is slightly different for Eu^{2+} and Dy^{3+}. This difference is responsible for a slight glow peak position shift if compared $SrAl_2O_4$:Eu,Dy and $SrAl_2O_4$:Dy.

As stated before, the important conditions for electron tunneling are: (I) the electron wave functions must overlap for electron initial and final state; (II) the energy of electron in initial and final state is equal. Experiments and corresponding calculations give confirmation that electron traps are located close to Eu^{3+} [64, 65, 68] and Dy^{4+} [76]. This suggests that wave function overlapping can take place and it is favorable for electron tunneling. The estimated energy levels for Eu and Dy ions in $SrAl_2O_4$ differ [35, 49, 77], therefore one can suggest the depth of electron traps could differ also. On the other hand it seems that initially both Eu and Dy in $SrAl_2O_4$ incorporate in charge states 3+ and the thermal treatment under reducing atmosphere leads to the formation of Eu^{2+}, but not the reduction of Dy^{3+}. The initial incorporation of Eu^{3+} and Dy^{3+} in $SrAl_2O_4$ requires charge compensation by host defects and since the charge states of both dopants are the same, the same host defects can be created. The electron traps - distorted tetrahedra of AlO_4 - are similar, however, not identical due to different Eu^{3+} and Dy^{4+} ion sizes and differently located energy levels of trapped electrons. The main problem for electron tunneling is the positions of energy levels of electron trap and the excited state of luminescence center. It can be noted the Eu^{2+} excitation spectrum is a complex wide band covering range from 2.76 eV up to 4,96 eV (450 nm – 250 nm) [40], the high frequency side of this band is due to charge transfer from oxygen to Eu, the low frequency side is determined by split 4f and 5d states of Eu, therefore, in accordance with ab initio calculations for two different cation sites [24, 78] there is a number of mutually closely located energy levels within ~ 1 eV interval. The study of Dy^{3+} doped YAG showed that there are 7 energy levels in the range 3.024 – 3.815 eV (with a difference of 0.79 eV) [71, 72]. This suggests that the similar closely located Dy levels could be present in $SrAl_2O_4$:Dy as well. Therefore, if the energy of electron located at a trap is within the mentioned energy range of Eu and Dy ions energy levels, the tunneling probability is substantial.

The prior discussion leads to the conclusion that observed luminescence bands peaking at 457 nm, 526 nm and ~572 nm in afterglow spectrum for $SrAl_2O_4$:Dy and at 520 nm band for $SrAl_2O_4$:Eu, Dy at 10 K arises from decay of excited Eu^{2+} and Dy^{3+} centers created via electron tunneling from host trap to Eu^{3+} and Dy^{4+} ions [75].

Another discovery when measuring $SrAl_2O_4$:Dy emission at 10 K temperature is the afterglow of this material at 576 nm (the more intense lines of Dy^{3+} luminescence). The afterglow intensity as well as its decay kinetics are dependent on duration of excitation, as it can be seen in Fig. 4.12. When using the logarythimc coordinates, decay kinetics can be approximated with a straight line – that again is strong evidence for the fact, that electron tunneling to the luminescence center takes place.

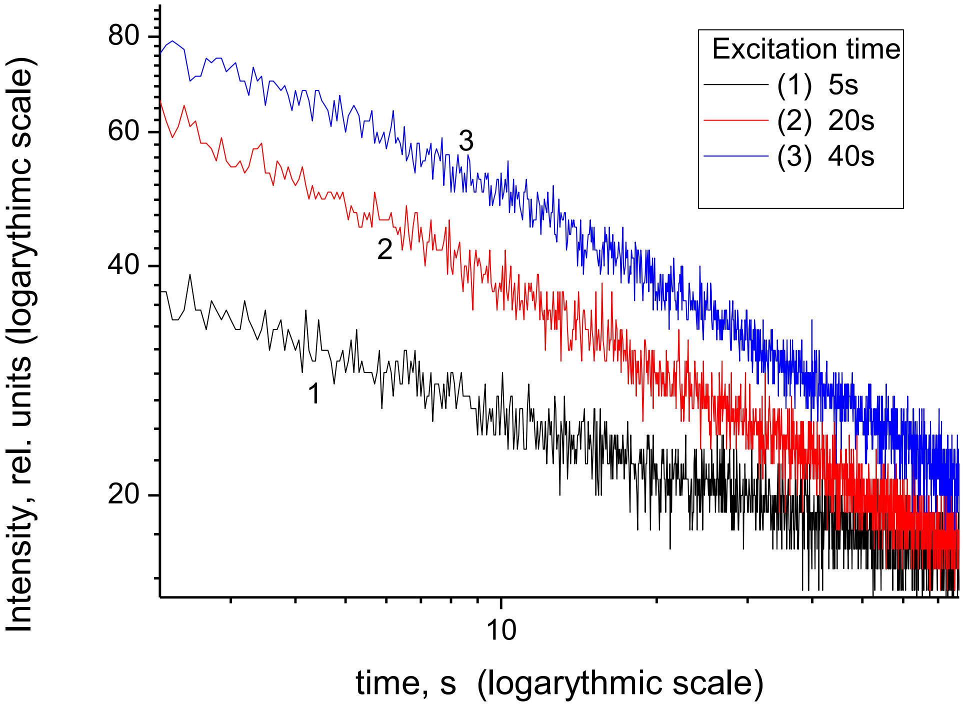

Fig. 4.12. The Dy^{3+} afterglow decay for different X-Ray excitation time intervals in logarythmic scale at 10K temperature

The luminescence kinetics dependence on excitation time is additional evidence to the fact that during excitation accumulation of trapped charges takes place. The afterglow of several minutes at 10 K is not due to thermal release of charge carriers from traps, as discussed beforehand. Therefore, the origin of this afterglow is the excited Dy^{3+} creation via electron tunneling. The TSL and afterglow are strong evidences that under X-ray irradiation the Dy^{3+} ions undergo a change of charge state. However, as described in [44] estimation of possible charge states of Dy in $SrAl_2O_4$ led the author of publication [44] to conclusion that Dy^{4+} and Dy^{2+} cannot exist in $SrAl_2O_4$. It should be pointed out that in the study of $SrAl_2O_4$:Eu,Dy under X-ray irradiation at 120 K the change of Eu^{2+} charge was observed, not any change of Dy^{3+} charge [44]. There has been a lot of discussion on this matter in literature overall and the results of our experiments are important since they strongly proves that electrons are trapped on some center that is not Dy and during irradiation by X-ray Dy^{3+} converts to Dy^{4+}.

4.5 $SrAl_2O_4$:Eu,Dy luminescence dependence on X-ray excitation duration

The author recorded the emission spectra of $SrAl_2O_4$:Eu,Dy under X-ray excitation and during TSL measurement as well as the afterglow spectra. The luminescence spectra of sample $SrAl_2O_4$:Eu,Dy at room temperature with different excitation time are shown in Fig. 4.13. The spectra reveal the intense Eu^{2+} luminescence band peaking at 526 nm, and three Dy^{3+} luminescence bands peaking at 576 nm, 664 nm, 754 nm. The Dy lines are not visible in photoluminescence spectrum. The Dy^{3+} band peaking at 483 nm is not resolved due to overlapping with the intense and a wide Eu^{2+} luminescence band. The shape of the spectrum changes during excitation and this could be due to gradual filling of traps by charge carriers. The luminescence intensity dependence on excitation time for several excitation intensities of X-Ray were recorded at RT and it was observed that Eu^{2+} luminescence intensity saturation is delayed relative to the beginning of excitation (Fig. 4.14.).

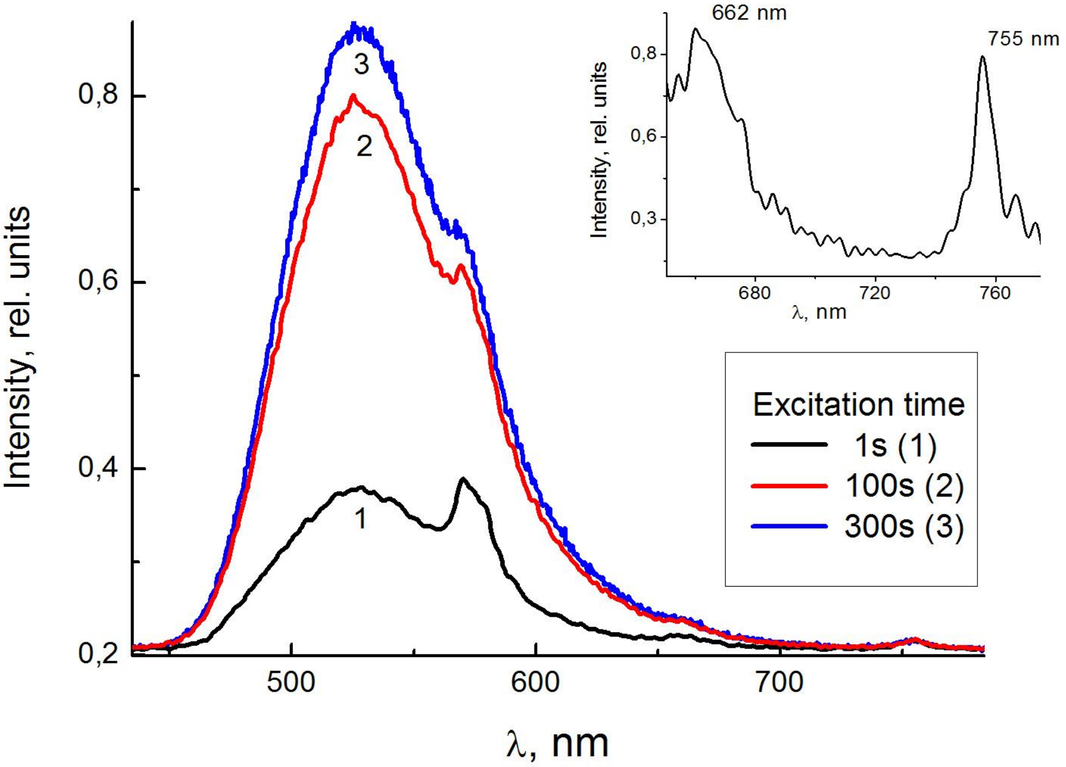

Fig. 4.13. X-ray excited uminescence spectra of $SrAl_2O_4$:Eu,Dy with different excitation duration at RT. Inset the 630 – 800 nm range in extended scale

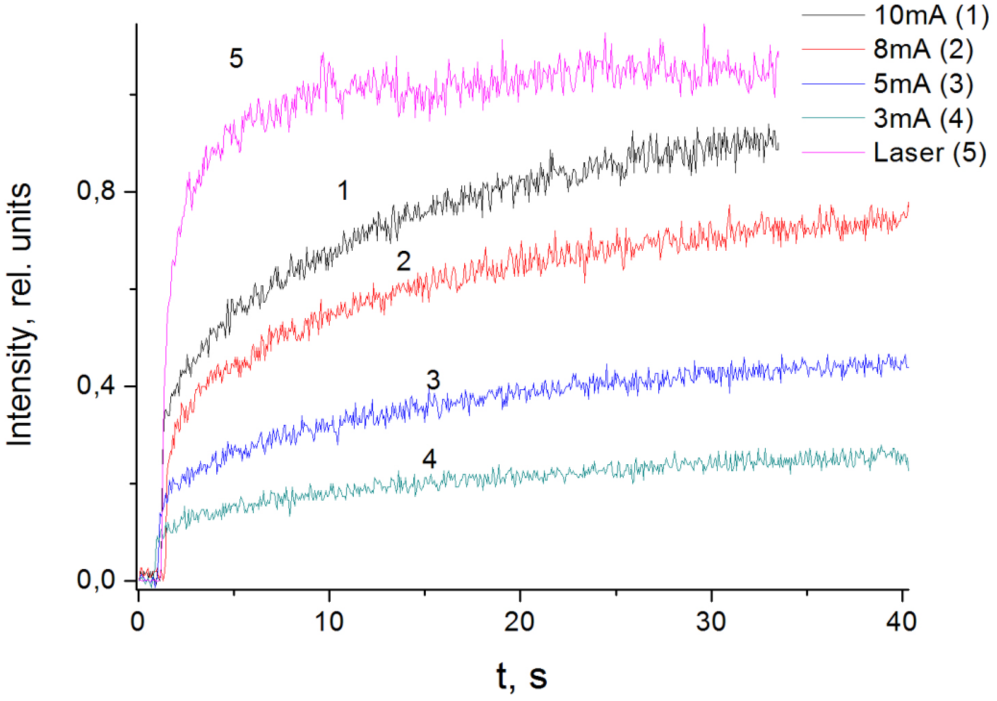

Fig. 4.14. The luminescence intensity at 526 nm dependence on excitation time at RT with different excitation intensities of X-Ray and laser (266 nm)

A similar luminescence intensity rise at RT was observed under UV excitation [68] as well as under X-ray excitation [44] and is explained as the thermally stimulated charge migration to the traps [44,68].

The analysis of luminescence spectra in Fig. 4.13. allowed to estimate that the changes of Dy^{3+} luminescence intensity during excitation are opposite to that observed for Eu^{2+} luminescence. The reason of this change is yet unclear and additional investigation is necessary. However, the results are evidence that trap filling affects the Dy^{3+} excitation, possibly these electron traps could be somewhat associated with Dy [75].

4.6 Luminescence of undoped $SrAl_2O_4$

The lack of information that can be found in publications on the luminescence of undoped $SrAl_2O_4$ is quite surprising, knowing that it might be helpful to acknowledge the defects that are responsible for the persistent luminescence process of the activated material. Most articles are concerned only with the doped material and do not deal with the luminescence of the undoped material at all. There are a couple of articles that do mention something on the undoped material – some of them report detecting no luminescence from the undoped material under UV excitation [28, 29]. Others describe a broad band emission with maximum at about 450 nm [79]. In [70] sharp lines in the photoluminescence spectrum were observed, that would usually not be characteristic for crystal intrinsic defects, presumably the origin of these emission lines could be a trace amount of transition metals or rare earths present in the material, as it is really difficult, even impossible to get rid of all the impurity ions in the precursor materials. Speaking of different excitation sources - a broad and complex luminescence band peaking at 450 and 500 nm was reported under X-ray excitation [31,32] that in authors opinion could be the luminescence of $SrAl_2O_4$ intrinsic defects. This, however, could be also due to trace amounts of Eu^{2+}, as these bands are very close to those known for Eu^{2+} in this material. Also,TSL of an undoped $SrAl_2O_4$ after excitation with electrons has been reported in [72], although the spectrum of the luminescence within glow peak has not been published, leaving a question – what kind of luminescence was detected and what defects might be present in the material to act as trapping as well as recombination centers. To deal with these unclarities and ambiguities, we have conducted a study on the luminescence of the undoped $SrAl_2O_4$ with different excitation sources and at different temperatures [62].

$SrAl_2O_4$ luminescence spectra at different temperatures were recorded. Fig. 4.15. shows photoluminescence spectra of the undoped sample under two different wavelengths of laser excitation at 10 K temperature. Although the luminescence is not strong, there is a clearly distinguishable wide asymmetrical shape band that can be decomposed to two bands peaking at 2.32 eV and 2.8 eV (534 and 442 nm) under 219 nm excitation and a 652 nm narrow peak under 311 nm excitation. This narrow line probably is emission from Mn^{4+} since in [81] is shown that these transient metal ions in $SrAl_2O_4$ polymorphs are responsible for lines within 652-657 nm and Mn is known as trace element in aluminum. As mentioned in [81], traces of transition metals are present even in material that has been synthesized from high purity grade precursor materials [64].

In search of the defects that are responsible for bands at 534 nm and 442 nm, the available information on defect luminescence in Al_2O_3 was checked. The luminescence of F– centers in pure α - Al_2O_3 is at ~440 nm (2.8 eV) [82-84], in turn the luminescence of F_2– centers is at 517 nm (2.4 eV) [85]. Important is to note that the F_2 – centers luminescence band position is found to be very close, even the same in both α - Al_2O_3 and γ - Al_2O_3 [86,87] showing weak influence from the structure. There is a strong possibility, that in the $SrAl_2O_4$ material these defects might be present as well and the F– centers and F_2– centers could be responsible for luminescence bands peaking at 442 nm and 534 nm.

The photoluminescence intensity at RT is low and equipment used was not sensitive enough for spectrum recording.

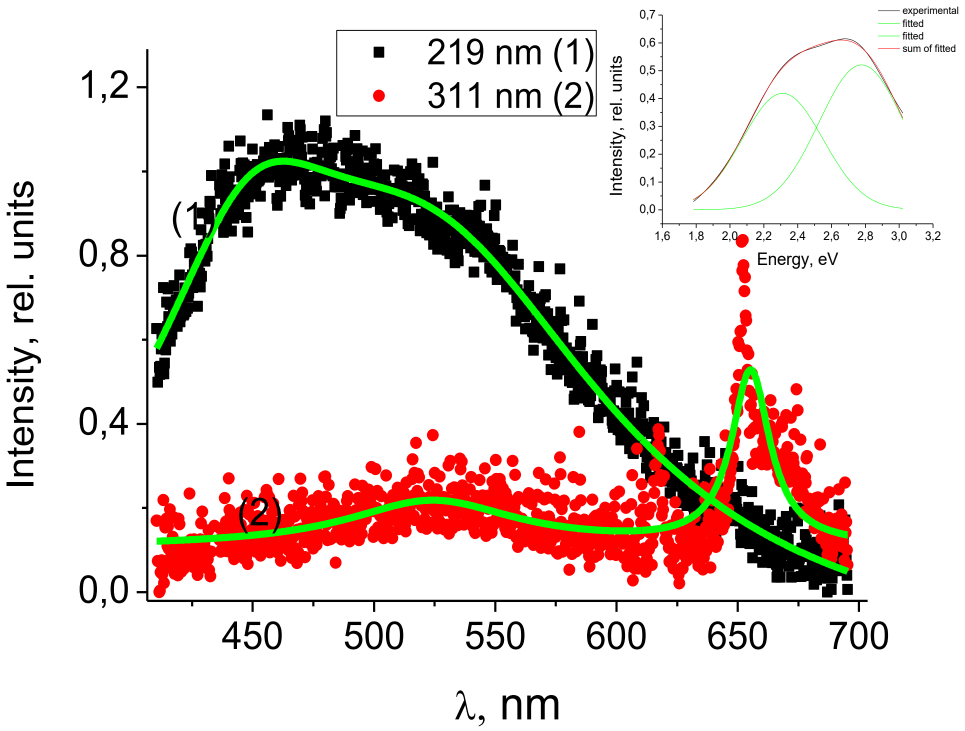

Fig. 4.15. Photoluminescence spectra of undoped $SrAl_2O_4$ at 10 K under different excitation wavelengths. Inset – fitted two peaks

Excitation spectra for two wavelengths were recorded – 650 nm, because there is a sharp maximum in the emission spectrum at this wavelength and at 505 nm, that is the maximum for the broad, complex band (although it could be decomposed in two bands for each of the overlapping maxima, this wavelength was chosen in order to ensure sufficient emission intensity for data recording). The excitation spectrum of photoluminescence (Fig. 4.16.) shows excitation energies within 210 - 330 nm (3.8 – 5.9 eV). These energies are well below the band gap of $SrAl_2O_4$ matrix. The band gap of $SrAl_2O_4$ is estimated to be around 6.5 eV [27], meaning that under laser excitation electron – hole pairs over the band gap were not created – therefore one can assume the presence of some defect levels in the band gap. Our equipment limits photoluminescence excitation spectra recording at wavelengths above 340 nm.

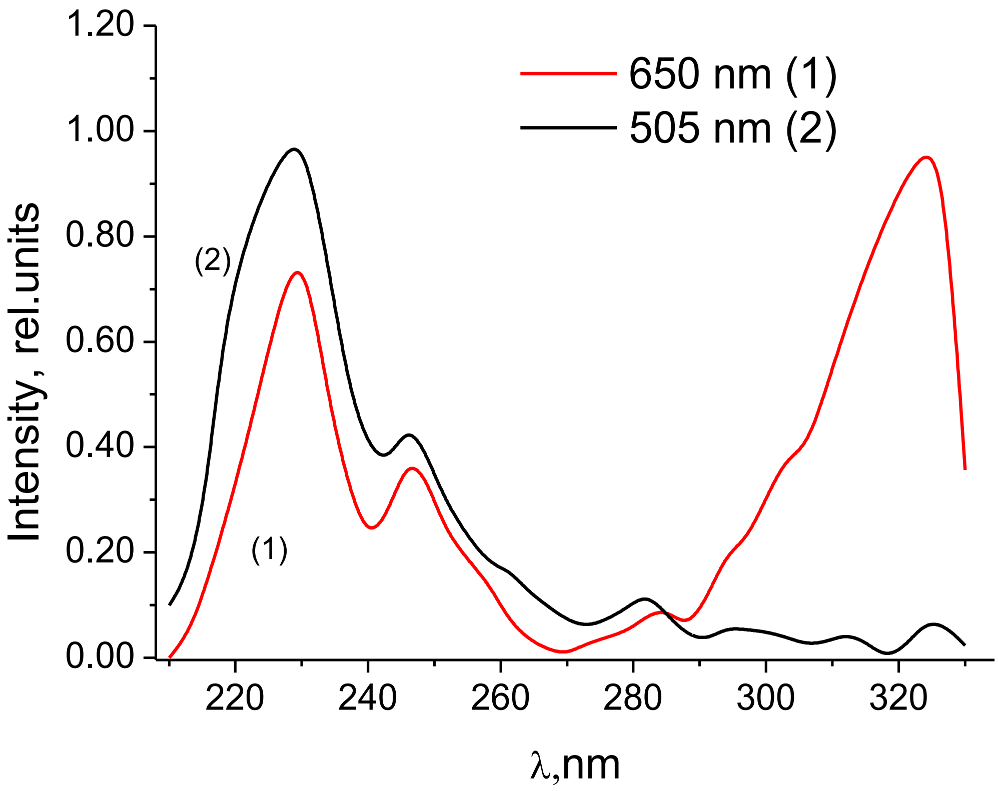

Fig. 4.16. Excitation spectra in two maxima of undoped $SrAl_2O_4$ emission

The 652 nm narrow band luminescence excitation peak close to the 325 nm could be related to Mn^{4+} excitation [81]. The two excitation peaks at ~230 nm and ~ 246 nm are common for the broad, complex luminescence band at 500 nm and for the narrow band at 652 nm. Since the F– centers are probably responsible for the broad band luminescence and Mn^{4+} - for the narrow band at 652 nm, the same excitation bands for both exclude the direct excitation of these centers, it can be assumed that energy transfer takes place. The possible hypothesis would be as follows. The initial step of excitation could be the charge transfer between oxygen and F– or F_2– center (excitation band peaking at ~229 nm), similar to that described for α- Al_2O_3 by Surdo et. al [82]. The other excitation band peaking at ~246 nm possibly is of the same nature, since both F- and F_2- centers could be involved. The step where energy is transferred to Mn^{4+} needs a separate study. Therefore, the photoluminescence spectra and corresponding excitation spectra show the intrinsic defects and trace impurity is present in $SrAl_2O_4$ sample. It will be noted the F- type centers can act as electron traps. The study of charge traps in $SrAl_2O_4$:Eu,Dy by Botterman et. al [68] showed that traps in vicinity of Eu ion are deeper than those at lager separation and it is possible that interaction of F- type centers with dopant ion changes the trap depth. Thus, the incorporation of dopant somewhat is related to defects in the host. Therefore, it is proposed the intrinsic defects are present also in rare earth doped $SrAl_2O_4$ and incorporation of Eu^{3+} as well as followed reduction to Eu^{2+} can strongly depends on the presence of F- type centers.

The excitation of undoped $SrAl_2O_4$ by 219 nm and 311 nm result in different luminescence spectra (Fig. 4.15.) The main differences are in the longer wavelength region of the spectra and in the luminescence intensity. In turn, under X-ray irradiation the luminescence spectrum at 10 K is more intense than that of photoluminescence and it was possible record the spectra at different temperatures (Fig. 4.17). There are clearly distinguishable maxima at 442 and 534 nm (similar that those in photoluminescence under laser excitation of 266 nm). These luminescence bands decrease in intensity due to thermal quenching at RT. The wide and intense luminescence band at low temperatures was recorded within 650 nm – 900 nm. This band quenches at RT; however, above 150 K a narrow band at 692 nm and a side band at 713 nm are revealed.

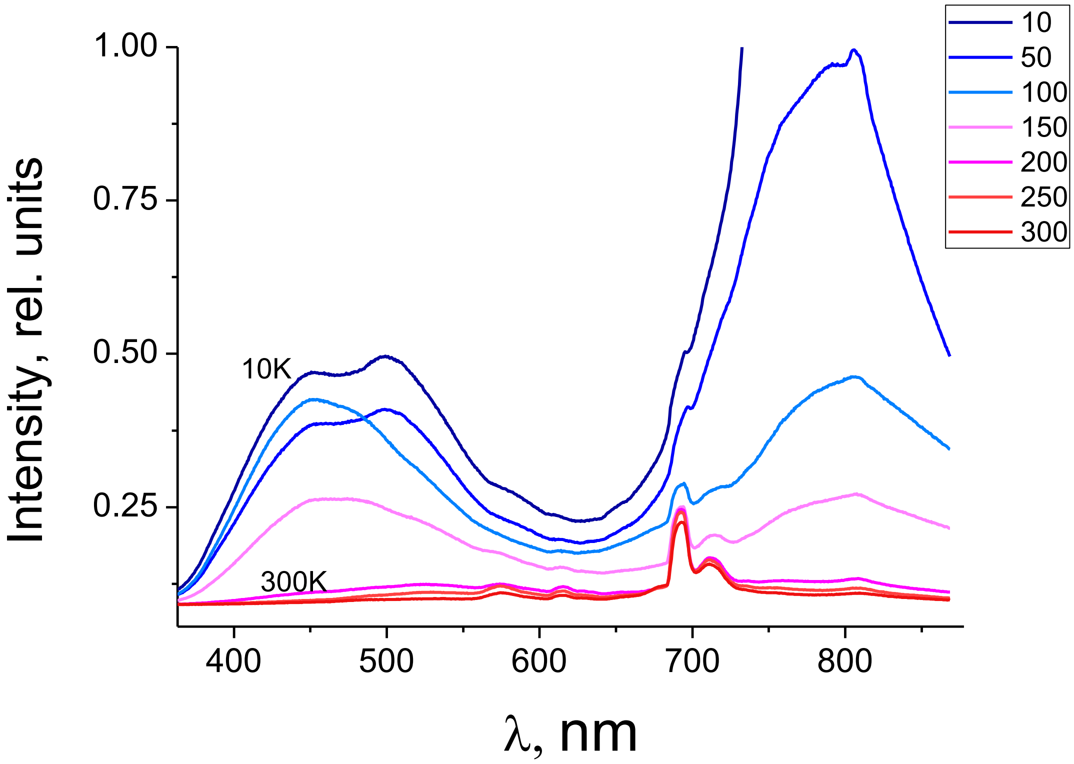

Fig. 4.17. X-ray induced luminescence of undoped $SrAl_2O_4$ at different temperatures (10-300 K).

The relative narrow luminescence bands of Cr^{3+} are known to be within 650 – 850 nm for several aluminates as well as for Al_2O_3 [88-90]. Therefore the narrow bands recorded at 692 nm and 713 nm under X-ray irradiation are due to spin-forbidden ^2E – $^4A_2$ transition in Cr^{3+}, at low temperature these narrow bands are strongly overlapped with more intense 790 nm band. The Cr usually present in aluminum, therefore Cr can be incorporated in $SrAl_2O_4$ from $Al(NO_3)_3·9H_2O$ that is used as the raw material in synthesis. The 790 nm band might also be attributed to Cr luminescence and this consideration is based on fact that in alkaline earth aluminate crystals Cr^{3+} ion substitutes two different crystallographic sites, that were already mentioned, if substituting for Sr^{2+} [91], and can substitute Al^{3+} as well, because the ionic radii of all the ions are quite similar. Therefore the X – ray excited luminescence confirms the presence of intrinsic defects responsible for overlapping bands between ~350 – 600 nm as well as presence of trace impurities in undoped $SrAl_2O_4$.

The electron – hole pairs were created in $SrAl_2O_4$ under X – ray irradiation and at low temperatures these charge carriers could be trapped, thus the TSL measurements were conducted. The TSL curves show a well resolved maximum at 100 K (Fig. 4.18.), that appears also in the $SrAl_2O_4$:Eu,Dy and $SrAl_2O_4$:Dy material, although it is shifted to 140 K in $SrAl_2O_4$:Eu,Dy. This can be attributed to the electrons release from intrinsic defects of the $SrAl_2O_4$ crystal. The weak glow peak was at ~260 K, at the same temperature the glow peak is in the rare earth doped $SrAl_2O_4$ [75]. The third well resolved peak is located above RT at around 400 K. This is also visible in the Eu and Dy doped material [63, 75], although this peak is slightly shifted to lower temperatures when adding the dopants. As glow peaks at the similar temperatures were observed in rare earth doped and undoped $SrAl_2O_4$, we would like to state that the defects that act as trapping centers in the long lasting luminescence of $SrAl_2O_4$:Eu,Dy are intrinsic defects nearby to the dopant, not the dopant impurities directly. The Dy co-doping clearly shifts the TSL peak at 400 K to a lower temperature [75], suggesting that the intrinsic defects could be perturbed by dopant or by trace impurities, thus contributing to more intensive afterglow.

Also, it is possible to see that the 790 nm peak exhibits an afterglow at low temperatures (Fig. 4.18.). It has already been stated in this work beforehand that tunneling luminescence is present in $SrAl_2O_4$ and this afterglow of Cr^{3+} might also be related to creation of excited Cr^{3+} via electron tunneling [62].

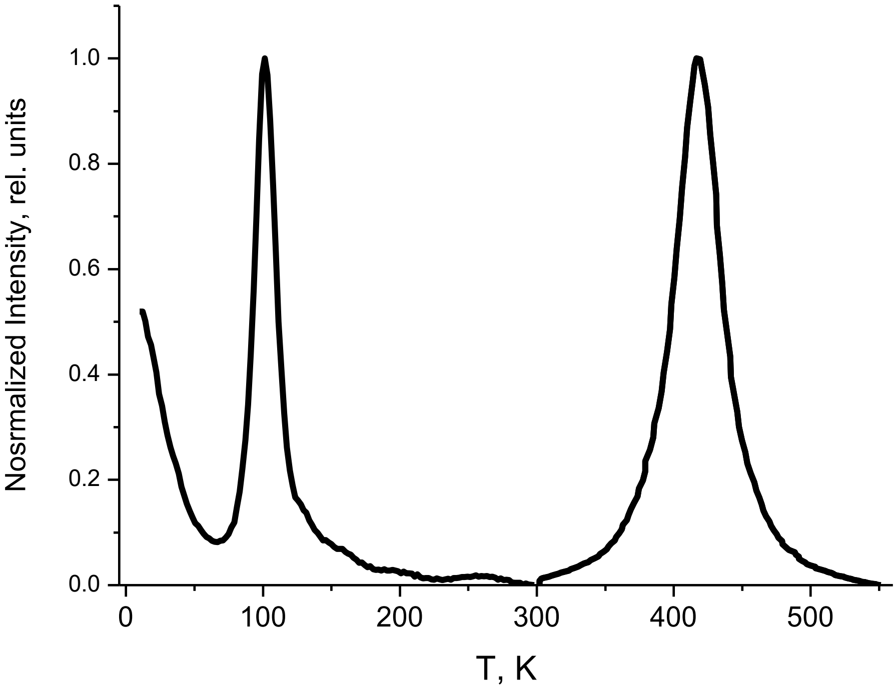

Fig. 4.18. TSL measurement for undoped $SrAl_2O_4$ at 790 nm (two measurements: 10-300 K and 300-700 K)

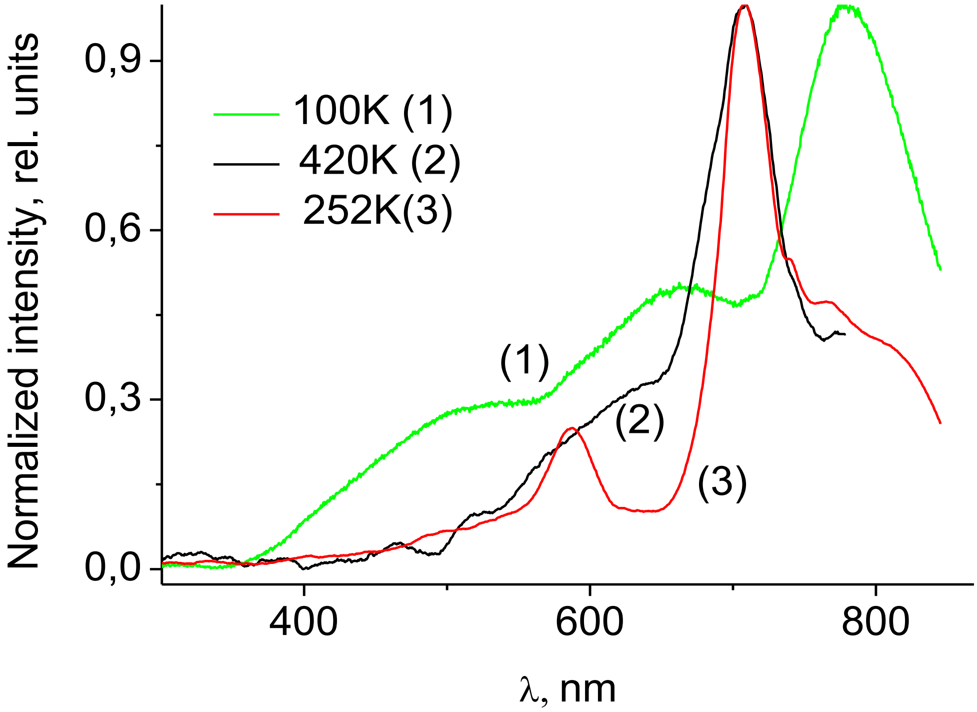

Fig. 4.19. Luminescence spectra undoped $SrAl_2O_4$ during TSL measurement at 100, 252 and 420 K.

The luminescence spectra within glow peaks at 100, 252 and 429 K (Fig. 4.19.), are different, however all of them can be explained with Cr and intrinsic defect luminescence. The spectrum recorded within 100 K glow peak reveals three broad luminescence bands peaking at 780 nm, 660 nm and around 500 nm. The long wavelength band is from Cr^{3+} spin-allowed transition $^4T_2$ – $^4A_2$ [92], the band at ~660 nm might be due to Cr^{3+} $^4T_2$ – $^4A_1$ transition, however other origin of this band cannot be excluded. The luminescence band peaking around 500 nm seems complex one however a good deconvolution on the components was not possible due to the strong overlap with the 660 nm band. As the luminescence band around 500 nm covers the same spectral range as X-ray induced luminescence bands of F– and F_2– centers (Fig. 4.19.) it could be that luminescence band around 500 nm is emerging from F–type centers. The support for this assumption is that F– centers luminescence was not quenched at 100 K (Fig. 4.17.). As mentioned above the relatively narrow Cr^{3+} luminescence bands were overlapped with strong band peaking at 790 nm. This 790 nm band partially undergoes quenching at RT, and the narrow Cr^{3+} bands became dominant (Fig. 4.17.). Within glow curve peaking at 252 K the before mentioned narrow Cr^{3+} luminescence bands are also dominant (Fig. 4.19.). The origin of luminescence band peaking at ~ 590 nm is unclear. Thus, the narrow Cr^{3+} bands in TSL spectra above 150 K are dominant and origin of this luminescence is the electron recombination with Cr^{4+}. The spectrum within glow curve above RT (420 K) shows similar features as the 252 K spectrum – with the Cr^{3+} emission as the dominant peak.

To summarize – the spectral measurements of undoped $SrAl_2O_4$ material under X-ray excitation up to RT show a clearly distinguishable luminescence. The luminescence of undoped $SrAl_2O_4$ consists of two main parts – trace impurity metals, namely, Mn^{4+} and Cr^{3+} luminescence, and luminescence of intrinsic defects – F- centers and F_2- centers. There is a strong possibility, that in the rare earth doped $SrAl_2O_4$ material these defects might be present as well and we propose that the presence of these defects is stimulating the Eu^{3+} ion incorporation. TSL shows two strong glow peaks – a peak under RT at around 100 K, emerging from intrinsic defects of the $SrAl_2O_4$ crystal and this peak also present in the doped materials, as well as a peak above RT at ~420 K, that might be attributed to the defects perturbed by trace impurities, and it is also present in the doped material, but its position depends on the dopant incorporated.

5. Conclusions

The study of luminescence of $SrAl_2O_4$, $SrAl_2O_4$:Dy and $SrAl_2O_4$:Eu,Dy was conducted at different temperatures under photoexcitation as well as under X-ray excitation. The analysis of results obtained allows to draw out the following conclusions.

1) The afterglow spectra for $SrAl_2O_4$:Eu,Dy excited at room temperature, 90 K and 10 K are alike - this indicates the luminescence center and its surroundings are the same at all temperatures studied.
2) The absence of glow maxima in $SrAl_2O_4$:Eu,Dy within the temperature range 10 – 50 K in thermally stimulated luminescence is strong evidence that electrons and holes are localized in traps and the origin of observed Eu, Dy and Cr ions afterglow luminescence within this temperature range is due to the creation of excited corresponding ions via electron tunneling process. This process is dominant within the low temperature range.
3) The thermally released charge migration is involved in excited Eu^{2+} creation at higher temperatures and it is possible that the tunneling of electron could be the last step of process even at higher temperature. The possible scheme is presented for mechanism responsible for long lasting luminescence: thermally released electron during migration can be multifold trapped and released. The last step of electron migration could be its direct trapping at Eu^{2+} excited state either trapping at deeper trap associated with Eu^{3+} and followed by excited Eu^{2+} creation via tunneling. The radiative decay of this excited Eu^{2+} state is the origin of persistent luminescence.
4) The line groups visible under X-ray excitation in $SrAl_2O_4$:Eu,Dy material along with the typical Eu^{2+} broad emission band are attributed to Dy^{3+} luminescence.
5) Both Eu and Dy luminescence peaks are observed in the afterglow and within glow curves of TSL measurement. Based on TSL and time resolved spectral measurements it is concluded, that under X-ray irradiation Eu^{2+} and Dy^{3+} serve as hole traps and the Eu^{3+} as well as Dy^{4+} are accumulated. Electron traps are located relative to Eu^{3+} and Dy^{4+} in such way, that electron tunneling probability is substantial.
6) The afterglow in low temperatures, TSL measurements and the charging of luminescence intensity imply that electron tunneling is present in both $SrAl_2O_4$:Eu,Dy and $SrAl_2O_4$:Dy, and luminescence afterglow at 10 K arises from decay of excited Eu^{2+} and Dy^{3+} centers created via electron tunneling from host trap to Eu^{3+} and Dy^{4+} ions.

7) The undoped $SrAl_2O_4$ material exhibits clearly distinguishable luminescence under X-ray excitation up to room temperature. The luminescence of undoped $SrAl_2O_4$ consists of two main parts – trace impurity metals, namely, Mn^{4+} and Cr^{3+} luminescence, and intrinsic defects luminescence – F- centers and F_2- centers. The intensities of broad bands of F-centers luminescence are low at room temperature due to partial quenching and therefore the narrow luminescence bands of Cr^{3+} are dominant. There is a strong possibility that these defects in the undoped $SrAl_2O_4$ material might be present in the rare earth doped $SrAl_2O_4$ as well and the author proposes that the presence of these defects is stimulating the Eu^{3+} ion incorporation.
8) TSL shows two strong glow peaks – a peak at ~ 100 K, emerging from intrinsic defects of the $SrAl_2O_4$ crystal and this peak, although shifted, is also presented in the doped materials, as well as a peak above RT at ~ 420 K, that might be attributed to the defects perturbed by trace impurities, and it is also present in the doped material, but the peak position depends on the dopant incorporated.

6. Thesis

1. The excited Eu^{2+} luminescence centers can be created in $SrAl_2O_4$:Eu,Dy via electron tunneling from a trap to Eu^{3+}. This led to the improvement of mechanisms stated in scientific publications for $SrAl_2O_4$:Eu,Dy persistent luminescence.

The new proposition is: thermally released electron during migration can be multifold trapped and released. The last step of electron migration could be its direct trapping at Eu^{2+} excited state either trapping at deeper trap associated with Eu^{3+} and followed by Eu^{2+} excited state creation via tunneling. The radiative decay of this state is the origin of persistent luminescence.

2. Under X-ray irradiation Eu^{2+} and Dy^{3+} serve as hole traps and the Eu^{3+} as well as Dy^{4+} are accumulated. Electron traps are located relative to Eu^{3+} and Dy^{4+} in such way, that electron tunneling probability is substantial.

Luminescence afterglow at 10 K arises from decay of excited Eu^{2+} and Dy^{3+} centers created via electron tunneling from host trap to Eu^{3+} and Dy^{4+} ions.

3. The undoped $SrAl_2O_4$ material exhibits clearly distinguishable luminescence under X-ray excitation up to room temperature. The luminescence of intentionally undoped $SrAl_2O_4$ consists of two main parts – trace impurity metals, namely, Mn^{4+} and Cr^{3+} luminescence, and intrinsic defects luminescence: F- centers and F_2- centers.

The experimental data and scientific proof of thesis 1. has been published in [64].

The experimental data and scientific proof of thesis 2. has been published in [75].

The experimental data and scientific proof of thesis 3. has been published in [62].

7. List of conferences and publications

7.1 Publications in chronological order

1. **Vitola V**., Millers D., Smits K., Bite I., Zolotarjovs A. **The search for defects in undoped $SrAl_2O_4$ material**, Optical Materials 87 (2019), 48-52.
2. Bite I., Krieke G., Zolotarjovs A., Auzins K., Laganovska K., **Liepina V**., Smits K., Grigorjeva L., Millers D., Skuja L. **Novel Method of Phosphorescent Strontium Aluminate Coating Preparation on Aluminium** Materials and Design 160 (2018), 794 – 802.
3. **Liepina V**., Millers D., Smits K., Zolotarjovs A. **X-ray excited luminescence of $SrAl_2O_4$:Eu,Dy at low temperatures**, Journal of Physics and Chemistry of Solids, 115 (2018), 381-385.
4. **Liepina V.**, Millers D., Smits K. **Tunneling luminescence in long lasting afterglow of $SrAl_2O_4$:Eu,Dy**, Journal of Luminescence, 185 (2017).
5. **Liepina V.**, Smits K., Millers D., Grigorjeva L., Monty C. **The luminescent properties of persistent strontium aluminate phosphor prepared by solar induced solid state synthesis**, IOP Conference Series Materials Science and Engineering (2012).

7.2 International conferences in chronological order

- Search for defects in $SrAl_2O_4$:Eu,Dy material, **Vitola Virginija**, Millers D, Smits K, Zolotarjovs A, Bite I, International Conference Functional materials and nanotechnologies, 2018, October 2 -5, Riga, Latvia.
- X-ray excited luminescence of $SrAl_2O_4$:Eu,Dy at low temperatures, **Vitola Virginija**, Millers D, Smits K, Zolotarjovs A, 7th International workshop on Photoluminescence in Rare Earths: Photonic Materials and Devices, 2017, November 30 – December 2, Rome, Italia (oral presentation).

- Low temperature luminescence studies in $SrAl_2O_4$:Eu,Dy, **Vitola Virginija**, Millers D, Smits K, Zolotarjovs A, Functional Materials and nanotechnologies 2017, April 24 – 27, Tartu, Estonia (oral presentation).
- Tunnelling luminescence studies in $SrAl_2O_4$:Eu,Dy, **Vitola Virginija,** Millers D, Smits K, Zolotarjovs A, International Young Scientists Conference Developments in Optics and Communications 2017, April 6 - 7, Riga, Latvia.
- The luminescent properties of persistent strontium aluminate phosphor prepared by solar induced solid state synthesis, **Liepina Virginija**, K.Smits, L.Grigorjeva, D.Millers, C. Monty, International Conference Functional Materials and nanotechnologies 2012, April 17 - 20, Riga, Latvia.

7.3 Local conferences in chronological order

- X-ray excited luminescence of SrAl2O4:Eu,Dy at low temperatures, **Virgīnija Vītola**, Donāts Millers, Krišjānis Šmits, Aleksejs Zolotarjovs, Ivita Bite**,** LU ISSP 33. scientific conference 2018, February 20 -22.
- Tunnelling luminescence in long lasting luminescent material $SrAl_2O_4$:Eu,Dy, **Liepina Virginija**, Millers D, Smits K, LU ISSP 33. scientific conference 2017, February 22 -24.
- The study of luminescence mechanism in $SrAl_2O_4$, **V.Liepina**, D. Millers, K. Smits, LU ISSP 31. scientific conference 2014, February 24 – 26.
- Luminescent properties of strontium aluminate **V.Liepina,** K.Smits, Dz.Jankovica, L.Grigorjeva, D.Millers, LU ISSP 29. scientific conference 2013, February 20 -22.
- Luminescent properties of rare earth activated aluminates, **V.Liepina,** K.Smits, L.Grigorjeva, D.Millers, LU ISSP 28. scientific conference 2012, February 08 – 10.
- The dependence of luminescent properties of synthesis parameters in strontium aluminates, **V.Liepiņa,** D.Jankoviča, K.Šmits, D.Millers, LU ISSP 27. scientific conference 2011, February 14 – 16.
- The synthesis and study of phosphorescent materials, **V.Liepina,** LU ISSP 26. scientific conference 2010, February 17 – 19.

8. Acknowledgements

The author is grateful for the support of the Laboratory of Solid State Radiation Physics – Krišjānis Šmits for advice on the research, Aleksejs Zolotarjovs and Krišjānis Auziņš for advice on the measurements and Ivita Bite for the synthesis and to all together for great working atmosphere. Special thanks to Dr. hab. Donats Millers for the outstanding support in the creation of this work and many lessons about life and physics during this time.

The author also wants to thank the Physics Departament of University of Latvia for the possibility to visit several scientific conferences and present this research.

This research project was supported financially by ERDF Project No: Nr.1.1.1.1/16/A/182 and ISSP Young Scientists project 2018.

References

[1] H. Hoppe, Recent developments in the field of inorganic phosphors, Angew. Chemie - Int. 48 (2009) 3572–3582. doi:10.1002/anie.200804005.

[2] M. Elsagh, M. Rajabi, E. Amini, Characterization of $SrAl_2O_4:Eu^{2+}$, Dy 3+ phosphor nano-powders produced by microwave synthesis route, J. Mater. Sci. Mater. Electron. 25 (2014) 1612–1619. doi:10.1007/s10854-014-1773-x.

[3] S.H. Kim, H.J. Lee, K.P. Kim, J.S. Yoo, "Spectral dependency of Eu^{2+}-activated silicate phosphors on the composition for LED application", Korean J. Chem. Eng. 23 (2006) 669–671. doi:10.1007/BF02706812.

[4] M. Sun, Z. Li, C. Liu, H. Fu, J. Shen, and H. Zhang, "Persistent luminescent nanoparticles for super-long time in vivo and in situ imaging with repeatable excitation," J. Lumin., vol. 145 (2013), 838–842. doi: 10.1016/j.jlumin.2013.08.070

[5] Y. William, S. Shionoya, H. Yamamoto, "Phosphor Handbook Second edition", CRC Press (2007) 27-77, New York

[6] K. Šaļimova," Pusvadītāju fizika", izdevniecība "Zvaigzne" (1979) 264-297, Rīga

[7] M. Fox, "Optical Properties of Solids", Oxford university press (2010) 247-267, New York

[8] F. Clabau, X. Rocquefelte, S. Jobic, P. Deniard, M.-H. Whangbo, A. Garcia, T. Le Mercier "Mechanism of Phosphorescence Appropriate for the Long-Lasting Phosphors Eu^{2+} -Doped $SrAl_2O_4$ with Codopants Dy^{3+} and B^{3+}," Chem. Mater. 17 (2005) 3904–3912. doi: 10.1021/cm050763r

[9] S. Han, X. Wang, Y. Wang, Y. Li "Determining the max effective trap depths of persistence luminescence by using trap depths continuous distributed phosphor" Opt. Mater. Express 5 (2015) 2377-2384

[10] T. Matsuzawa," A New Long Phosphorescent Phosphor with High Brightness", $SrAl_2O_4:Eu^{2+},Dy^{3+}$, J. Electrochem. Soc. 143 (1996) 2670. doi:10.1149/1.1837067

[11] P. Smet, N. Avci, K. Van den Eeckhout, D. Poelman, “Extending the afterglow in $CaAl_2O_4$:Eu,Nd persistent phosphors by electron beam annealing”, Optical Materials Express 2, 10. (2012) 1306-1313. doi: 10.1364/OME.2.001306

[12] Z. Jingxian, X. Qin, L. Yingliang, “Synthesis and characterization of needle-like $BaAl_2O_4$:Eu,Dy phosphor via hydrothermal-homogeneous precipitation method”Journal of Rare Earths, 31, 4. (2013) 342

[13] Y. Lin, Z. Tang, Z. Zhang, C. W. Nan, “Anomalous luminescence in $Sr_4Al_{14}O_{25}$:Eu, Dy phosphors”, Appl. Phys. Lett. 81, 996 (2002), doi: 10.1063/1.1490631

[14] D. Singh, V. Tanwar, A. P. Simantilleke, S. Bhagwan, B. Mari, P. S. Kadyan, K. Chander, S. Singh “Synthesis and enhanced luminescent characterization of $SrAl_4O_7$:Eu^{2+},RE^{3+} (RE = Nd, Dy) nanophosphors for light emitting applications” J Mater Sci: Mater Electron 27 (2016), 5303. doi: 10.1007/s10854-016-4428-2

[15] B. Lei, Y. Liu, J. Liu, Z. Ye, C. Shi “Pink light emitting long-lasting phosphorescence in Sm^{3+}-doped $CdSiO_3$” Journal of Solid State Chemistry, 177,4-5 (2004), 1333–1337. doi: 10.1016/j.jssc.2003.11.006

[16] Y. Zhu, M. Ge “Study on the emission properties of $Sr_2MgSi2O_7$:Eu,Dy for luminous fiber application” J Mater Sci: Mater Electron 25 (2014), 5512. doi: 10.1007/s10854-014-2337-9

[17] R. Pang, C. Li, Q. Su, L. Shi “A novel blue-emitting long-lasting proyphosphate phosphor $Sr_2P_2O_7$:Eu^{2+},Y^{3+}” journal of physiscs and Chemistry of Solids, 70, 2. (2009) 303-306. doi: 10.1016/j.jpcs.2008.10.016

[18] H. Y. Wu, Y. H. Hu, Y.H. Wang, C. J. Fu, F. W. Kang "Synthesis of Eu^{2+} and Dy^{3+} Codoped $Ba_2MgSi_2O_7$ Phosphor for Energy Storage", Advanced Materials Research 236-238 (2011), 3028-3031.

[19] Y. Lin, Z. Zhang, Z. Tang, X. Wang, J. Zhang, Z. Zheng, “Luminescent properties of a new long afterglow Eu^{2+} and Dy^{3+} activated $Ca_3MgSi_2O_8$ phosphor”, Journal of the European Ceramic Society, 21,5 (2001) 683–685. doi:10.1016/s0955-2219(00)00252-1

[20] Y. Lin, Z. Tang, Z. Zhang, C. W. Nan, “Luminescence of Eu^{2+} and Dy^{3+} activated $R_3MgSi_2O_8$-based (R = Ca, Sr, Ba) phosphors” J. Alloy. Compd. 348 (2003) 76–79, doi: 10.1016/S0925-8388(02)00796-X

[21] M.Y. Lin, S. Chen, Z. Chen, J.Q. Zou, G.D. Xu, M. M. Wang, C. Q. He, J. H. Zhang, X.F. Yu, “Preparation and luminescence property of Eu^{2+}, Mn2+ co-doped silicates phosphors for white LED” Journal of Alloys and Compounds, 632 (2015), 756–759, doi: 10.1016/j.jallcom.2015.01.270.

[22] Y. Li, M. Gecevicius, Q. Jianrong “Long phosphorescent phosphors: From fundamentals to applications”, Chemical Society Reviews, (2016) Manuscript ID: CS-SYN-07-2015-000582.R2

[23] Y. Chang, J. Hsiang, M. Liang “Phase Evolution During Formation of $SrAl_2O_4$ from $SrCO_3$ and α-Al_2O_3/AlOOH” Journal of the American Ceramic Society, 90, 9 (2007), 2759–2765. doi:10.1111/j.1551-2916.2007.01831.x

[24] M.Nazarov, M.G.Brik, D.Spassky, B.Tsukerblate, A.Nor Nazida, M.N.Ahmad-Fauzi “Structural and electronic properties of $SrAl_2O_4:Eu^{2+}$ from density functional theory calculations”, Journal of Alloys and Compounds, 573, 6-10 (2013), doi: 10.1016/j.jallcom.2013.04.004

[25] T. Nakamura, K. Kaiya, T. Takahashi, T. Matsuzawa, M. Ohta, C. Rowlands, C. G. Smith, P. Riedi, Phys. Chem. Chem. Phys. 3 (2001), 1721.

[26] T. Nakamura, K. Kaiya, N. Takahashi, T. Matsuzawa, C. C. Rowlands, V. Beltran-Lopez, G. M. Smith, P. C. Riedif “High frequency EPR of europium(II)-doped strontium aluminate phosphors” J. Mater. Chem. 10 (2000) , 2566, doi: 10.1039/B004061O

[27] J. Holsa, T. Laamanen, M. Lastusaari, J. Niittykoski, P. Novak, “Electronic structure of the $SrAl_2O_4:Eu^{2+}$ persistent luminescence material”, J Rare Earth, 27 (2009), 550-554. doi: 10.1016/S1002-0721(08)60286-0

[28] C. dos S. Bezerra, A. B. Andrade, P. J. R. Montes, M. V. do. S. Rezende, and M. E. G. Valerio, “The effects of cooling rate on the structure and luminescent properties of undoped and doped $SrAl_2O_4$ phosphors,” Opt. Mater. (Amst)., 72 (2017) 71–77. doi:10.1016/j.optmat.2017.05.044

[29] H. Terraschke, M. Suta,M. Adlung, S. Mammadova, N. Musayeva, R. Jabbarov, M. Nazarov, C. Wickleder, “$SrAl_2O_4:Eu^{2+}$, Dy^{3+} Nanosized Particles : Synthesis and Interpretation of Temperature-Dependent Optical Properties,” J. Spectrosc., 2015 (2015). doi:10.1155/2015/541958

[30] P. Yang, M.K Lu, C. F. Song, S. W. Liu, D. Xu, D. R. Yuan, X. F. Cheng “Preparation and tunable photoluminescence characteristics of Ni2+:$SrAl_2O_4$,” Opt. Mater. (Amst)., 24 (2003), 575–580. doi: 10.1016/S0925-3467(03)00147-2

[31] D. Nakauchi, G. Okada, M. Koshimizu, and T. Yanagida, “Storage luminescence and scintillation properties of Eu-doped $SrAl_2O_4$ crystals,” J. Lumin., 176 (2016) 342–346. doi: 10.1016/j.jlumin.2016.04.008

[32] D. Nakauchi, G. Okada, M. Koshimizu, and T. Yanagida, “Optical and scintillation properties of Nd-doped $SrAl_2O_4$ crystals,” J. Rare Earths, 34, 8 (2016), 757–762. doi: 10.1016/S1002-0721(16)60090-Xv

[33] H. Terraschke, M. Suta, M. Adlung, S. Mammadova, N. Musayeva, R. Jabbarov, M. Nazarov, C. Wickleder, “$SrAl_2O_4$:Eu^{2+}(,Dy^{3+}) Nanosized Particles: Synthesis and Interpretation of Temperature-Dependent Optical Properties” Journal of Spectroscopy, 2015 (2015). doi: 10.1155/2015/541958

[34] M. Ayvacıklı, A. Ege, and N. Can, “Radioluminescence of $SrAl_2O_4$: Ln^{3+} (Ln = Eu, Sm, Dy) phosphor ceramic,” Opt. Mater. (Amst)., 34 (2011), 138–142. doi: 10.1016/j.optmat.2011.07.023

[35] P. Dorenbos, “Mechanism of Persistent Luminescence in Eu^{2+} and Dy^{3+} Codoped Aluminate and Silicate Compounds,” J. Electrochem. Soc., vol. 152, 7 (2005), H107. doi: 10.1149/1.1926652

[36] P. Dorenbos “The 5d level positions of the trivalent lanthanides in inorganic compounds” Journal of Luminescence, 91, 3-4 (2000), 155-176. doi: 10.1016/S0022-2313(00)00229-5

[37] P. Dorenbos “Locating lanthanide impurity levels in the forbiden band of host crystals” J. Lumin. 108 (2004), 01-305 doi: 10.1016/j.jlumin.2004.01.064

[38] P. Dorenbos “Energy of the first 4f7 - 4f65d transition of Eu^{2+} in inorganic compounds” J. Lumin. 104, (2003), 239-260. doi:10.1016/S0022-2313(03)00078-4

[39] F. Clabau, X. Rocquefelte, S. Jobic, P. Deniard, M.-H. Whangbo, A. Garcia, T. Le Mercier “On the phosphorescence mechanism in $SrAl_2O_4$:Eu^{2+} and its codoped derivatives,” Solid State Sci., 9 (2007), 608–612. doi: 10.1016/j.solidstatesciences.2007.03.020

[40] K. Van den Eeckhout, P. F. Smet, D. Poelman, “Persistent Luminescence in Eu^{2+}-Doped Compounds: A Review,” Materials (Basel)., vol. 3, 4 (2010), 2536–2566. doi:10.3390/ma3042536

[41] V. Liepina, K. Smits, D. Millers, L. Grigorjeva, C. Monty “The luminescent properties of persistent strontium aluminate phosphor prepared by solar induced solid state synthesis” IOP Conference Series Materials Science and Engineering 38, 1 (2012), 12-45. doi: 10.1088/1757-899X/38/1/012045

[42] I. Bite, G. Krieke, A. Zolotarjovs, K. Laganovska, V. Liepina, K. Smits, L. Grigorjeva, D. Millers, L. Skuja “Novel Method of Phosphorescent Strontium Aluminate Coating Preparation on Aluminium” Materials and Design (2018) 160 (2018), 794 – 802. doi: 10.1016/j.matdes.2018.10.021

[43] E. Shafia, A. Aghaei, A. Davarpanah, M. Bodaghi, M. Tahriri, S. H. Alavi, “Synthesis and Characterization of $SrAl_2O_4:Eu^{2+}$, Dy^{3+} Nanocrystalline Phosphorescent Pigments” Trans. Ind. Ceram. Soc., 70, 2 (2011) 71-77.

[44] K. Korthout, K. Van den Eeckhout, J. Botterman, S. Nikitenko, D. Poelman, and P. Smet, “Luminescence and Xray absorption measurements of persistent $SrAl_2O_4$:Eu,Dy powders: evidence for valence state changes,” Phys. Rev. B 84,8 (2011), 085140.

[45] T. Aitasalo, J. Holsa, M. Lastusaari, H. Jungner, J. Niittykoski, “Mechanisms of persistent luminescence in Eu^{2+}, RE^{3+} doped alkaline earth aluminates,” J. Lumin., 94–95 (2001), 59–63. doi: 10.1016/S0022-2313(01)00279-4

[46] T. Aitasalo, P. Deren, J. Holsa, H. Jungner, J.C. Krupa, M. Lastusaari, J. Legendziewicz, J. Niittykoski, W. Strek, Persistent luminescence phenomena in materials doped with rare earth ions, J. Solid State Chem. 171 (2003) 114–122. doi:10.1016/S0022-4596(02)00194-9.

[47] T. Aitasalo, J. Hölsä, H. Jungner, J.-C. Krupa, M. Lastusaari, J. Legendziewicz, “Effect of temperature on the luminescence processes of $SrAl_2O_4:Eu^{2+}$”, Radiat. Meas. 38 (2004) 727–730.

[48] T. Aitasalo, A. Durygin, J. Hölsä, M. Lastusaari, J. Niittykoski, A. Suchocki “Low temperature thermoluminescence properties of Eu^{2+} and R^{3+} doped CaAl2O4” Journal of Alloys and Compounds, 380, 1-2 (2004), 4-8.

[49] F. Clabau, X. Rocquefelte, S. Jobic, P. Deniard, M.-H. Whangbo, A. Garcia, T. Le Mercier "Mechanism of Phosphorescence Appropriate for the Long-Lasting Phosphors Eu^{2+} -Doped $SrAl_2O_4$ with Codopants Dy^{3+} and B^{3+}," Chem. Mater., 17 (2005), 3904–3912. doi: 10.1021/cm050763r

[50] J. Hölsä, H. Jungner, M. Lastusaari, J. Niittykoski, Persistent luminescence of Eu^{2+} doped alkaline earth aluminates, MAl_2O_4:Eu^{2+}, J. Alloys Compd. 323-324 (2001) 326–330. doi:10.1016/S0925-8388(01)01084-2.

[51] Y. Chang, H. Hsiang, M. Liang "Characterizations of Eu, Dy co-doped $SrAl_2O_4$ phosphors prepared by the solid-state reaction with B2O3 addition", Journal of Alloys and Compounds, 461, 1-2 (2008), 598-603. doi: 10.1016/j.jallcom.2007.07.078Get

[52] C. Chang, Z. Yuan, D. Mao "Eu^{2+}activated long persistent strontium aluminate nano scaled phosphor prepared by precipitation method", Journal of Alloys and Compounds, 415, 1-2 (2006). doi: 10.1016/j.jallcom.2005.04.219

[53] B. Rao, D. Mukherjee, B.Reddy "Novel approaches for preparation of nanoparticles", Nanostructures for Novel Therapy Synthesis, Characterization and Applications, Micro and Nano Technologies, 1 (2017), 1-36. doi: 10.1016/B978-0-323-46142-9.00001-3

[54] Q Xiao, L. Xiaou, Y. Liu, X. Chen, Y. Li "Synthesis and luminescence properties of needle-like $SrAl_2O_4$:Eu, Dy phosphor via a hydrothermal co-precipitation method" Journal of Physics and Chemistry of Solids 71, 7 (2010), 1026-1030. doi: 10.1016/j.jpcs.2010.04.017

[55] H. Wu, Y. Jin "Luminescence of divalent europium activated spinels synthesized by combustion and the enhanced afterglow by dysprosium incorporation", Physica B: Condensed Matter 488 (2016), 8-12. doi: 10.1016/j.physb.2016.02.012

[56] Y. Lin, Z. Tang, Z. Zhang, "Preparation of long-afterglow Sr4Al14O25-based luminescent

material and its optical properties". Mater. Lett. 51 (2001), 14–18. doi: 10.1016/S0167-577X(01)00257-9

[57] A. Alvani, F, Moztarzadeh, A. Sarabi, "Effects of dopant concentrations on phosphorescence properties of Eu/Dy-doped Sr3MgSi2O8". J. Lumines, 114 (2005), 131–136, doi: doi.org/10.1016/j.jlumin.2004.12.012

[58] G .Zatryb, A. Podhorodecki, J. Misiewicz, J. Cardin, F. Gourbilleau "On the nature of the stretched exponential photoluminescence decay for silicon nanocrystals", Nanoscale Res. Lett., 6, 1 (2011), 106. doi: 10.1186/1556-276X-6-106

[59] E. Kotomin, V. Kuzovkov, "Modern Aspects of Diffusion-Controlled Reactions: cooperative phenomena in bimolecular processes", Elsevier Sci. 34 (1996).

[60] A. Bos, "Thermoluminescence as a Research Tool to Investigate Luminescence Mechanisms", Materials 10,12 (2017), 1357. doi: 10.3390/ma10121357

[61] McKeever S., "Theory of Thermoluminescence and Related Phenomena", World, Scientific Publishing (1997), 74-186., Singapure

[62] V. Vitola, D. Millers, K. Smits, I. Bite, A. Zolotarjovs "The search for defects in undoped $SrAl_2O_4$ material", Optical Materials, 87 (2019), 48-52 doi: 10.1016/j.optmat.2018.06.004

[63] T. Katsumata, R. Sakai, S. Komuro, T. Morikawa, "Thermally Stimulated and Photostimulated Luminescence from Long Duration Phosphorescent $SrAl_2O_4$:Eu, Dy Crystals", J. Electrochem. Soc. 150 (2003) H111. doi:10.1149/1.1565141.

[64] V. Liepina, D. Millers, K. Smits "Tunneling luminescence in long lasting afterglow of $SrAl_2O_4$:Eu,Dy" J. Lumin., 185 (2017), 151-154. doi:10.1016/j.jlumin.2017.01.011

[65] H. Hagemann, D. Lovy, S. Yoon, S. Pokrant, N. Gartmann, B. Walfort, J. Bierwagen, "Wavelength dependent loading of traps in the persistent phosphor $SrAl_2O_4$:Eu^{2+}, Dy^{3+}," J. Lumin., 170 (2015), 299–304. doi: 10.1016/j.jlumin.2015.10.035

[66] M. Jain, B. Guralnik, M.T. Andersen, Stimulated luminescence emission from localized recombination in randomly distributed defects, J. Phys. Condens. Matter. 24 (2012) 385-402. doi:10.1088/0953-8984/24/38/385402.

[67] G. Kitis, V. Pagonis, Properties of thermoluminescence glow curves from tunneling recombination processes in random distributions of defects, J. Lumin. 153 (2014) 118–124. doi:10.1016/j.jlumin.2014.03.014.

[68] J. Botterman, J. J. Joos, and P. F. Smet, "Trapping and detrapping in SrAl2 O4:Eu,Dy persistent phosphors: Influence of excitation wavelength and temperature," Phys. Rev. B - Condens. Matter Mater. Phys., 90, 8 (2014), 1–15. doi: 10.1103/PhysRevB.90.085147

[69] W. Jia, H. Yuan, L. Lu, H. Liu, and W. M. Yen, “Phosphorescent dynamics in $SrAl_2O_4$: Eu^{2+}, Dy^{3+} single crystal fibers,” J. Lumin., 3, 97, (1998), 0–4. doi: 10.1016/S0022-2313(97)00230-5

[70] P. J. R. Montes, M. E. G. Valerio, “Radioluminescence properties of rare earths doped $SrAl_2O_4$ nanopowders,” J. Lumin. 130 (2010), 1525–1530. doi: 10.1016/j.jlumin.2010.03.024Get

[71] P. J. R. Montes, M. E. G. Valerio, M. V. S. Rezende, “Mechanisms of radioluminescence of rare earths doped $SrAl_2O_4$ and Ca12Al14O33 excited by X-ray,” J. Electron Spectros. Relat. Phenomena, 189 (2013), 39–44. doi: 10.1016/j.elspec.2013.06.011

[72] M. Ayvacıklı, A. Ege, N. Can, “Radioluminescence of $SrAl_2O_4$: Ln3+ (Ln = Eu , Sm , Dy) phosphor ceramic,” Opt. Mater. (Amst). 34 (2011), 138–142. doi: 10.1016/j.optmat.2011.07.023

[73] G. Raju, H. Jung, J. Park, J. Chung, B. Moon, J. Jeong, S. Son, J. Kim., “Sintering temperature effect and luminescent properties of Dy^{3+} : YAG nanophosphor,” J. Optoelectron. Adv. Mater., 12, 6 (2010), 1273–1278.

[74] G. S. Raju, J. Park, H. Jung, B. Moon, J. Jeong, J. Kim, “Luminescence properties of Dy^{3+} : $GdAlO_3$ nanopowder phosphors,” Curr. Appl. Phys., 9 (2009), 92–95.

[75] V. Liepina, D. Millers, K. Smits, A. Zolotarjovs, I. Bite, “X-ray excited luminescence of $SrAl_2O_4$:Eu,Dy at low temperatures” J. Phys. Chem. Solids, 115 (2017), 381–385. doi: 10.1016/j.jpcs.2017.12.040

[76] T. Takeyama, T. Nakamura, N. Takahashi, M. Ohta, “Electron paramagnetic resonance studies on the defects formed in the Dy (III) -doped $SrAl_2O_4$,” Solid State Sci. 6 (2004), 345–348. doi: 10.1016/j.solidstatesciences.2004.02.001

[77] E. Nakazawa and T. Mochida, “Traps in SrA1204 : Eu^{2+} phosphor with rare-earth ion doping,” J. Lumin. 74 (1997), 236–237.

[78] M. Nazarov, M.G. Brik, D. Spassky, B. Tsukerblat, “Crystal field splitting of 5d states and luminescence mechanism in $SrAl_2O_4$:Eu2þ phosphor”, J. Lumin. 182 (2017), 79–86. https://doi.org/10.1016/j.jlumin.2016.10.015.

[79] B. Di Bartolo and X. Chen, "Advances in energy transfer processes," Proceedings of the 16th Course of the International School of Atomic and Molecular Spectroscopy, (1999).

[80] P. Yang, M.K Lu, C. F. Song, S. W. Liu, D. Xu, D. R. Yuan, X. F. Cheng "Preparation and tunable photoluminescence characteristics of $Ni^{2+}:SrAl_2O_4$," Opt. Mater. (Amst)., 24 (2003), 575–580. doi: 10.1016/S0925-3467(03)00147-2

[81] P. Boutinaud, D. Boyer, A. Perthue, R. Mahiou, E. Cavalli, M.G. Brik, "Spectroscopic investigations of $SrAl_2O_4$ polymorphs" J.Lumin, 159 (2015), 158-165. doi: 10.1016/j.jlumin.2014.11.006

[82] A.I. Surdo, V.S. Kortov, V.A. Pustovarov, "Luminescence of F and F+ centers in corundum upon excitation in the interval from 4 to 40 eV", Radiat. Meas., 33 (2001), 587–591. doi: 10.1016/S1350-4487(01)00064-6

[83] M. Luca, N. Coron, C. Djuardin, H. Kraus, V.B. Mikhailik, M. A. Verdier, P.C.F. Di Stefano, "Scintillating and optical spectroscopy of Al_2O_3:Ti for dark matter searches", Nucl Instrum Methods Phys Res A, 606 (2009), 545-551. doi: 10.1016/j.nima.2009.04.034

[84] J. Valbis, N. Itoh, "Electronic excitations, luminescence and lattice defect formation in α-Al2O3 crystals", Radiat. Eff. Defects Solids, 116 (1991), 171–189. doi: 10.1080/10420159108221357

[85] M.Itou, A.Fujivara and T.Uchino, "Reversible Photoinduced Interconversation of Color Centers in α - Al_2O_3 Prepared under Vacuum", J.Phys.Chem. C, 113 (2009), 20949 - 20957. doi: 10.1021/jp908417m

[86] B.D. Evans, G.J. Pogatshnik, Y. Chen, "Optical properties of lattice defects in α-Al_2O_3", Nucl. Instruments Methods Phys. B, 91 (1994), 258–26. doi: 10.1016/0168-583X(94)96227-8

[87] M.Baronskiy, A.Rastorguev, A.Zhuzhgov, A.Kostyukov, O.Krivoruchko, V.Snytnikov, "Photoluminescence and Raman spectroscopy studies of low-temperature γ-Al_2O_3 phases

synthesized from different precursors", Opt. Mater., 53 (2016), 87–93. doi: 10.1016/j.optmat.2016.01.029

[88] V.Singh, G.Sivaramaiah, J.L.Rao, S.Sripada, S.H. Kim, "An electron paramagnetic resonance and optical study of Cr doped $BaAl_{12}O_{19}$ powders", Ceramics International, 40 (2014), 9629 – 9636. doi: 10.1016/j.ceramint.2014.02.043

[89] J.Križan, J.Možina, I.Bajsic, M.Mazaj, "Synthesis and Fluorescent Properties of Chromium-Doped Aluminate Nanopowders", Acta Chim. Slov., vol.59, pp.163-168, 2012.

[90] M.N.Trindade, R.M.F.Scalvi, L.V.A.Scalvi, "Cr^{3+} Distribution in Al1 and Al2 Sites of Alexandrite ($BeAl_2O_4$:Cr^{3+}) Induced by Annealing, Investigated by Optical Spectroscopy", Energy and Power Engineering(2010) 18-24, doi:10.4236/epe.2010.21004

[91] W. Strek, P. Dere, B. Jezowska-Trzebiatowska. "Broad-band emission of Cr^{3+} in $MgAl_2O_4$ spinel" Journal de Physique Colloques, 48 (1987), 475 - 477, doi: 10.1051/jphyscol:19877113

[92] X.Li, G.Jiang, S.Zhou, X.Wei, Y.Chen, C.K.Duan, M.Yin. "Luminescent properties of chromium(III)-doped aluminate for temperature sensing", Sensors and Actuators B, 202 (2014), 1065-1069, 2014. doi: 10.1016/j.snb.2014.06.053